ISSN 0024-8266

mnassa

monthly notes of the astronomical society of southern africa

Volume 82 Nos 1-2 February 2023

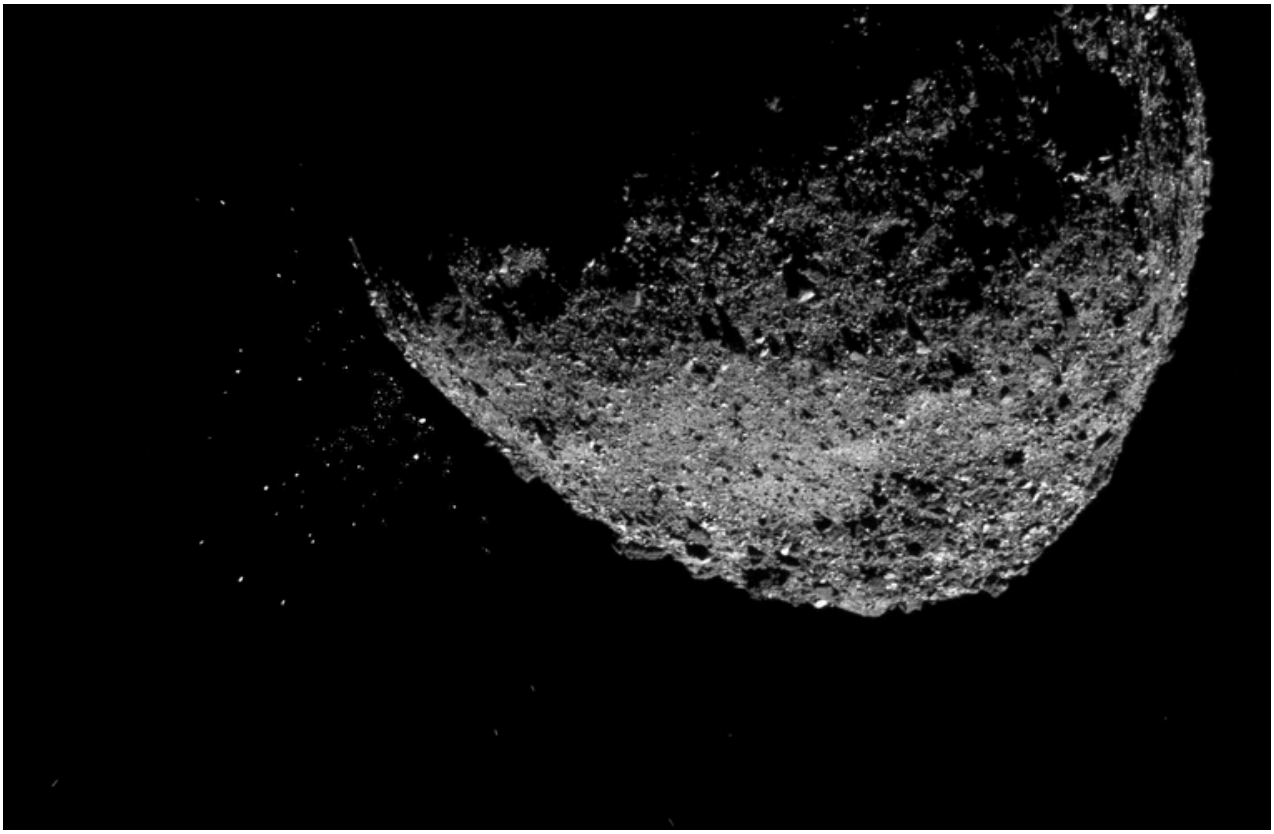

In this issue:

News Notes
Asteroid Bennu
Improving Dobsonian Bearings
Darkness and Colour of Lunar eclipses
Recent Colloquia
Streicher Asterisms

Cover photo: A composite image of a short and long exposure photograph of Asteroid Bennu showing the largest particle ejection on January 6, 2019. Photograph: NASA/Goddard/University of Arizona/Lockheed Martin (See P3).

Astronomical Society of Southern Africa
ASSA
Est. 1922

mnassa

Vol 82 Nos 1-2 **February 2023**

News Note: Royal Astronomical Society announces all journals to publish as open access from 2024

In a move that will be welcomed by researchers both professional and amateur, the Royal Astronomical Society (RAS) has announced that all the journals it publishes will be Open Access (OA) from January 2024. This move will enable everyone in the global community to have free, immediate, and unrestricted access to the research that they publish. *Monthly Notices of the Royal Astronomical Society (MNRAS), Monthly Notices of the Royal Astronomical Society Letters (MNRASL),* and *Geophysical Journal International* (GJI) will join *RAS Techniques and Instruments* (RASTI), a new journal launched by the Society in 2021, in being fully OA. The RAS journals portfolio will continue to publish alongside *Astronomy & Geophysics*, the RAS's magazine for its Fellows, which will see no change.

All articles published in the RAS journals portfolio, from the very first volumes published in 1827 to the latest articles, will be free to read in their entirety. As the scientific community works ever harder to ensure barriers to cutting edge science are eliminated, facilitating openness, dissemination, and reproducibility of impactful academic research, the Society is excited to be a key contributor to the open science movement, helping to drive discoverability and change.

With this move to OA the journals will no longer charge subscription fees and will instead be supported by Article Processing Charges (APCs), with the infrastructure to ensure that authors continue to face no financial barrier to publishing their science in the RAS journals.

News Note: International Team Announces Discovery of Super-Hot Stars Using Southern African Large Telescope

Using the largest single optical telescope in the Southern Hemisphere, an international team of astronomers has discovered eight of the hottest stars in the universe, all with surfaces hotter than 100,000 degrees. The work has been published in *Monthly Notices of the Royal Astronomical Society.*

The paper is based on data gathered using the Southern African Large Telescope (SALT), the largest single optical telescope in the southern hemisphere, with a 10m x 11m mirror. The study describes how a survey of helium-rich subdwarf stars led to the discovery of several very hot white dwarf and pre-white dwarf stars, the hottest of which has a surface temperature of 180,000 degrees Celsius. For comparison, the Sun's surface is a mere 5,800 degrees.

One of the stars identified is the central star of a newly discovered planetary nebula, which is one light year in diameter. Two of the others are pulsating, or 'variable' stars. All of these stars are at an advanced stage of their life cycle and are approaching the end of their lives as white dwarfs. Due to their extremely high temperatures, each of these new discoveries is more than one hundred times brighter than the Sun, which is considered unusual for white dwarf stars.

White dwarfs are roughly the same size as planet Earth, but a million times more massive, with masses closer to that of the Sun's. They are the densest stars in existence that consist of normal matter. Pre-white dwarfs are a few times bigger and will shrink to become white dwarfs within a few thousand years.

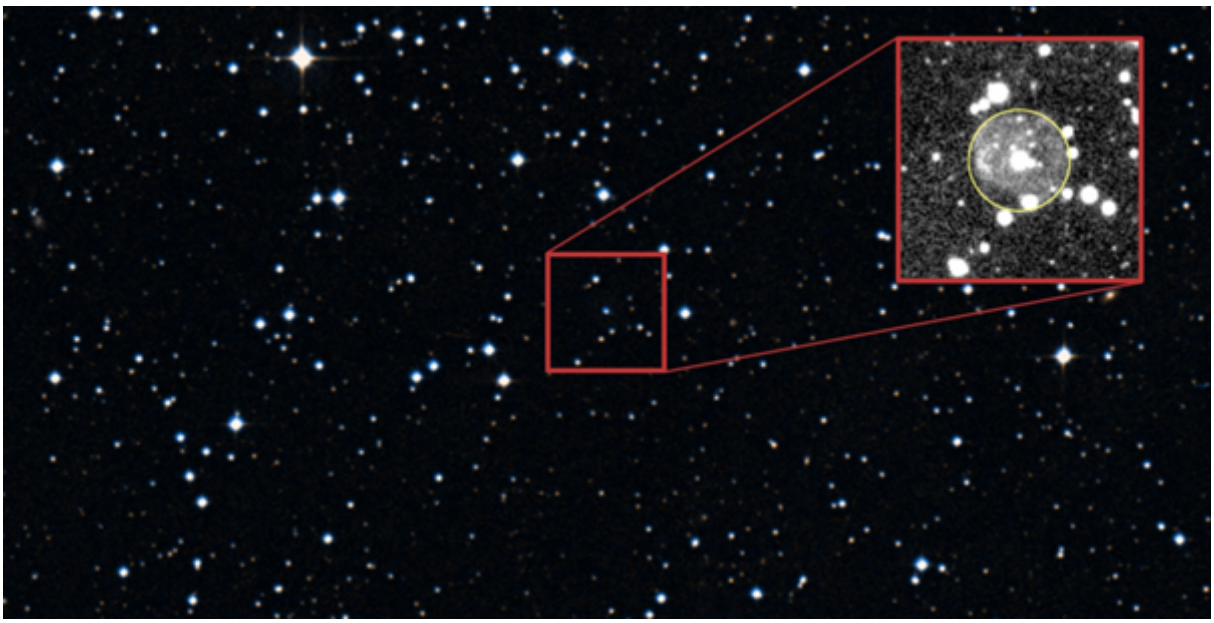

Fig 1. A sky survey image centred on the newly-discovered O(H) star SALT J203959.5-034117 (J2039). Credit: Tom Watts (AOP), STScINASA, The Dark Energy Survey.

Simon Jeffery, an astronomer at the Armagh Observatory and Planetarium, who led the research, said that stars with effective temperatures of 100 000°C or higher are incredibly rare. It was a real surprise to find so many of these stars in our survey. These discoveries will help to increase our understanding of the late stages of stellar evolution and they demonstrate that SALT is a fantastic telescope for our project. He added that it had been exciting to work with an experienced team, who collectively enabled the discovery of the stars, the analysis of their atmospheres, and the discovery of pulsations and a nebula in a very short space of time.

The University of Tuebingen's Professor Klaus Werner, who co-authored the paper, was proud to have helped develop this ground-breaking research. The discovery of eight very hot white dwarf and pre-white dwarf stars and a new planetary nebula is hugely significant, and we hope that these findings will help to shed new light on the formation of our galaxy.

Dr Itumeleng Monageng, of the Department of Astronomy, University of Cape Town, and South African Astronomical Observatory, said it was an honour to have played a part in this incredible discovery. The SALT survey of helium-rich hot subdwarfs was intended to explore evolutionary pathways amongst groups of highly evolved stars. It is fascinating to have discovered eight new extremely hot stars in the process, one of which is surrounded by a planetary nebula.

Ref: Jeffery, C.S. et al, *MNRAS* **519,** 2321, 2023

The 2022 campaign to observe potential meteors from asteroid Bennu

Tim Cooper and Magda Streicher

Introduction

Asteroid 101955 Bennu is an Apollo-type asteroid, which have orbits larger than the Earth's but the perihelion distance q is inside Earth's orbit at its aphelion ($a \geq 1.0$ and $q \leq 1.017$ AU). In the case of Bennu, a = 1.126, q = 0.897, and the asteroid orbits with a period of 1.20 years in an orbit inclined a little over 6° to the ecliptic plane. As such the orbit is able to come within a minimum orbit intersection distance (MOID) of only 0.003 AU from Earth's orbit at closest approach. The asteroid was the target of the OSIRIS-REx probe which launched on 8 September 2016, and arrived at Bennu on 3 December 2018. Shortly after arrival the spacecraft captured images of solid particles ejected from the surface of the asteroid (see Figure 1). Subsequently, the probe collected samples from the asteroid using its Touch-And-Go Sample Acquisition Mechanism (TAGSAM), and which will be returned to Earth for analysis, scheduled to arrive on 24

September 2023. Sample analysis will give more information on the chemical and physical properties of the dust, which can be correlated with the properties of any observed meteors in the future.

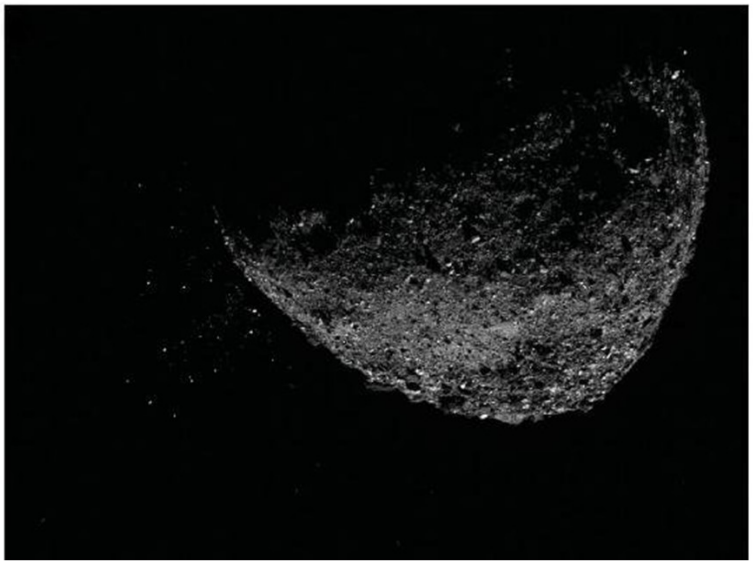

Fig 1. Solid particles ejected from the surface of the asteroid (To left in this photo from OSIRIS-Rex).

Given that Bennu is ejecting dust from its surface, particles ejected in the past may potentially result in a meteor shower if they enter Earth's atmosphere. Ye (2019) first pointed to the possibility of meteor activity, and that particles ejected from the surface of Bennu since 1500 CE should already be starting to cross Earth's orbit. Any activity of faint, slow moving meteors would be expected to occur around 25 September from a radiant at R.A. 00h20 (005°), Decl. -34°, in the constellation of Sculptor. Cooper (2019) observed for 13.0 hours during the period 22-26 September 2019, noting that activity was below the sporadic background. Nevertheless the observations that year set a useful baseline for future observations. The potential meteor shower from Bennu has also been the target for the global Cameras for All-sky Meteor Surveillance (CAMS) network between 2019 and 2021. Results by Jenniskens et al (2022) concluded no compact activity from near the predicted radiant, but several meteor orbits were determined which might be due to activity from much older ejecta. Seeing that meteor activity from Bennu is possible, and that occasional outbursts from meteor streams do occur, we intend to continue observations into the future, even if only to characterise the background activity against which future observations can be compared. For these reasons the authors observed again in 2022. Note all times are in UT, and positions are given for J2000.0. All observations were carried out from a dark sky site in Limpopo Province.

Other meteor radiants possibly active during September

With any meteor shower where activity is expected to be low, it is important to plot all meteors seen in order to identify other streams which might be active and to avoid errors in assigning observed meteors to specific radiants. Even so, when plotting meteors from radiants in close proximity, it may be hard to differentiate the true source by plotting alone, and for this reason it is important to also note the apparent speed of the plotted meteors. Meteors from Bennu are expected to emanate from a radiant at R.A. 11h20 (005°), Decl. -34°, and with a geocentric velocity of 6 km/sec would

characteristically appear to be very slow moving. Therefore meteors seen to radiate at or from nearby the Bennu radiant, but observed to be fast-moving, would not be recorded as Bennu meteors. Table 1 lists meteor radiants known to be active around the same time as any activity from Bennu, and includes the Taurids and Orionids which are annual showers, as well as some showers which are not active each and every year, but may show periodic activity.

*Table 1. Expected shower radiants and IAU shower codes. *Note BEN and RAD1 are not official shower codes and are used only in this report to identify potential meteors from the listed positions. Vg is the geocentric velocity of shower members in km/sec.*

Shower	Code	R.A. (°)	Decl. °	Vg (speed)
Bennu	BEN*	00h20 (005)	–34	6 (very slow)
Northern Taurids	NTA	00h26 (007)	+10	28 (slow)
Southern Taurids	STA	00h46 (011)	+03	27 (slow)
September epsilon-Perseids	SPE	03h34 (054)	+40	65 (fast)
Orionids	ORI	04h20 (065)	+17	67 (fast)
nu-Eridanids	NUE	05h00 (075)	+06	67 (fast)
56-Cetids	FCE	01h56 (029)	–23	45 (medium)
upsilon-Cetids	UCE	02h34 (039)	–03	61 (fast)
Radiant 1 from 2019	RAD1*	23h54 (358)	–29	medium-slow

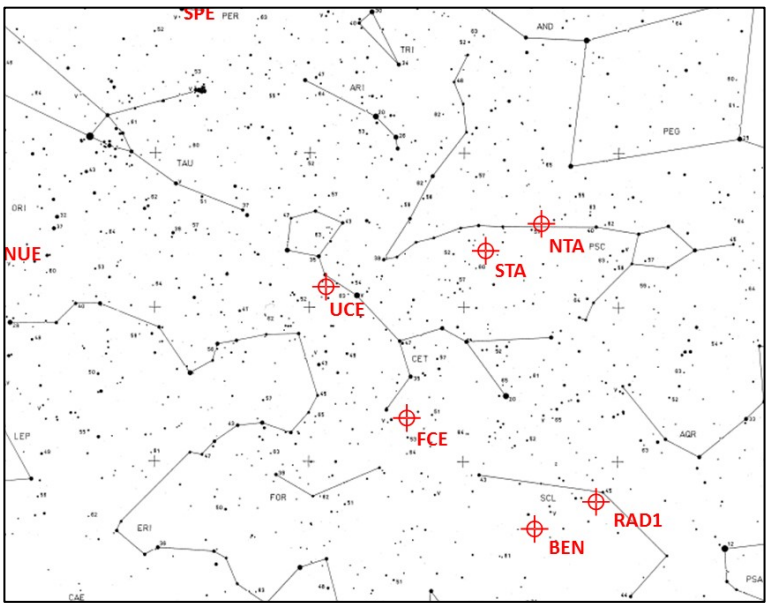

Fig 2. Positions of radiants in the vicinity of, and with period of activity overlapping with the potential radiant from asteroid Bennu (BEN). The radiants are STA = Southern Taurids, NTA = Northern Taurids, UCE = upsilon-Cetids, SPE = September epsilon-Perseids, NUE = nu-Eridanids, FCE = 56-Cetids, RAD1 = possible radiant identified from 2019 observations (see Cooper 2019).

The positions of all possible centres of meteor activity listed in Table 1 are shown in Figure 2. During 2019 observations, several meteors were seen to emanate from a possible centre nearby the Bennu radiant and determined to be around R.A. = 23h54

(358.5°), Decl. -29.4°, close to the magnitude 4.5 star delta Sculptoris. Eight of these were observed during the night of September 25/26, with five observed in the 30 minute interval from 1856-1926 UT. All meteors were recorded as slow to medium speed. These are identified as RAD1, and a watch was kept out for them again during the 2022 campaign.

Observations during the 2022 campaign

The authors planned to observe between 21 and 26 September. Unfortunately the nights of 21/22 and 22/23 September were clouded out, but observations were carried out during the nights of 23/24 to 25/26 September without cloud interference. There was no interference from the Moon. Watch times and numbers of meteors observed are given in Tables 2 and 3. All meteors were plotted on Gnomonic Atlas Brno 2000.0 charts (Znojil 1988).

Table 2. Observations by Magda Streicher. T_{eff} = effective observing time after correcting for breaks, LM=limiting magnitude. Shower codes as in Table 1.

Date 2022	Time UT	T_{eff} hours	LM	BEN	STA	RAD1	SPO	Total
Sep 23/24	1851-1953	1.03	5.8	1		1	2	4
Sep 23/24	2005-2106	1.02	5.8				3	3
Sep 23/24	2106-2206	1.00	5.8				5	5
Sep 24/25	1845-1945	1.00	6.0				9	9
Sep 24/25	1945-2045	1.00	6.0				7	7
Sep 24/25	2058-2158	1.00	6.0		2	1	8	11
Sep 25/26	1900-2000	1.00	6.0	1?			9	10
Sep 25/26	2023-2046	0.38	6.0				1	1
Total		**7.43**		**2?**	**2**	**2**	**44**	**50**

Table 3. Observations by Tim Cooper. T_{eff} = effective observing time after correcting for breaks, LM=limiting magnitude. Shower codes as per Table 1. Shower codes as per Table 1.

Date 2022	Time UT	T_{eff} hours	LM	BEN	STA	NUE	FCE	RAD1	SPO	Total
Sep 23/24	1851-1951	1.00	5.80						4	4
Sep 23/24	1952-2052	1.00	5.85					1	4	5
Sep 23/24	2113-2213	1.00	5.90		1				6	7
Sep 24/25	1830-1930	1.00	6.30	1					5	6
Sep 24/25	1935-2035	1.00	6.25	1	1				4	6
Sep 24/25	2058-2147	0.82	6.20	1			1	1	9	12
Sep 24/25	0121-0221	1.00	6.10			1			2	3
Sep 25/26	1857-1937	0.67	6.35						4	4
Sep 25/26	1942-2042	1.00	6.35		2				7	9
Total		**8.49**		**3**	**4**	**1**	**1**	**2**	**45**	**56**

Magda Streicher observed for 7.43 hours, seeing fifty meteors, forty four sporadic meteors, two Taurids, and two which aligned with the Bennu radiant, see plots 3 and 38 shown in Figure 3. In addition Magda recorded two meteors aligned with RAD1, see plots 2 and 28 shown in Figure 4.

Tim Cooper observed for 8.49 hours, seeing fifty six meteors. Most of these were sporadic meteors, as well as four Taurids, one nu-Eridanid and one 56-Cetid. Only two possible members were aligned with the Bennu radiant, see plots 14 and 19 shown in Figure 3. One meteor was seen on 23 September at 19h26 in peripheral vision moving away towards the right, which could be traced back very roughly to the Bennu radiant. Since the path could not be determined with certainty it was recorded as sporadic. Note however this is the same meteor seen by Magda as her plot 3, which is aligned with the Bennu radiant in Figure 3.

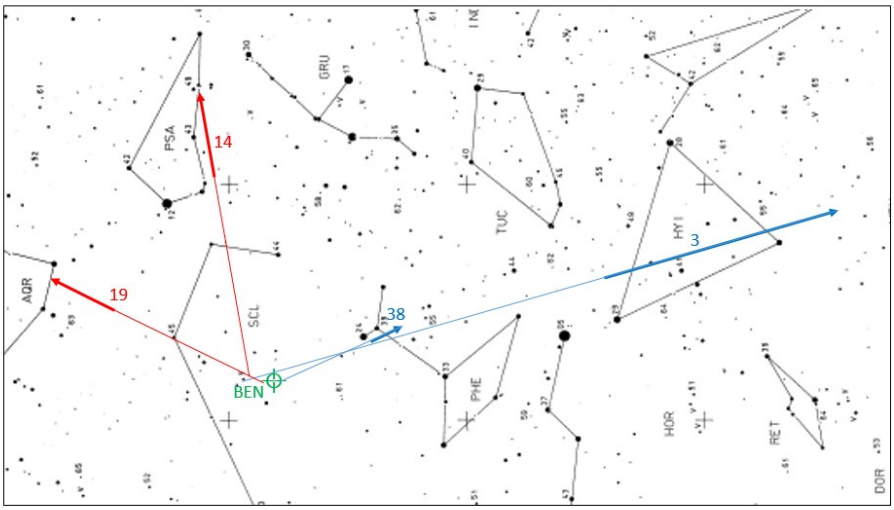

Fig 3. Four meteors possibly aligned with Bennu radiant. Meteors plotted by Magda Streicher shown in blue, meteors plotted by Tim Cooper shown in red.

In addition Tim recorded two meteors aligned with RAD1, see plots 7 and 26 shown in Figure 4.

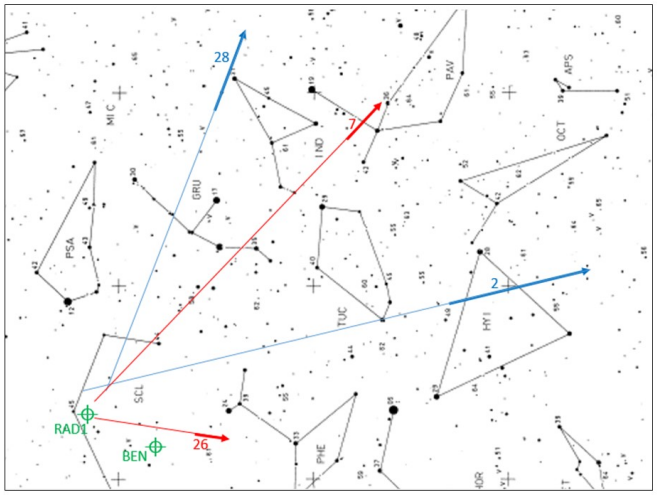

Fig 4. Four meteors possibly aligned with RAD1 radiant. Meteors plotted by Magda Streicher shown in blue, meteors plotted by Tim Cooper shown in red.

Discussion

During the combined 15.92 hours observation, only four meteors were observed which aligned with the Bennu radiant. They are plotted in Figure 3 and had the following appearance times and properties:

23 September, 19h26, Streicher, Plot 3, magnitude -1, very slow speed.
24 September, 19h03, Cooper, Plot 14, mag 2, yellow, very slow, fragmentary appearance.
24 September, 19h38, Cooper, Plot 19, mag 3, white, slow, fragmentary appearance.
25 September, 19h01, Streicher, Plot 38, magnitude 3-4, slow.

Both meteors recorded by Tim as BEN occurred on September 24 at 19h03 and 19h38, and were noticeably different in appearance from all other meteors observed during the campaign, displaying a fragmentary or sparkling appearance along their path. Both were also recorded as very slow moving. The significance of these facts is as yet unverified, but if indeed these were meteors from Bennu, the activity would correspond to a zenithal hourly rate (ZHR) around 4.8 centred on solar longitude ($\lambda_{\odot}$) 181.42°. Outside this period, the activity was indistinguishable from the sporadic background.

Also during the 16 hours observations, four meteors were plotted which showed reasonable alignment with the potential centre plotted in 2019 as RAD1, as shown in Figure 4. The appearance times and properties of these four meteors were:

23 September, Streicher, Plot 2, 19h24, magnitude 3-4, medium speed.
23 September, 20h49, Cooper, Plot 7, mag 3, white, medium.
24 September, Streicher, Plot 28, 21h05, magnitude 1-2, fast.
24 September, 21h16, Cooper, Plot 26, mag 5, white, slow.

The differences in apparent speeds, from slow to fast, makes it unlikely that these are all related, and we conclude any alignment is most likely coincidental and that any activity from RAD1 seen in 2019 cannot be confirmed.

Conclusions

Based on 16 hours visual observations by the authors we conclude any activity of potential meteors from asteroid Bennu in 2022 was indistinguishable from the sporadic background. The occurrence of two meteors on September 24 around solar longitude 181.42°, both very slow moving and fragmentary in appearance is nevertheless interesting. As in 2019, no significant activity of potential meteors from asteroid Bennu

was observed in 2022, but the results are useful as they set a baseline for the current epoch against which future observations can be compared.

References

Cooper, T. P. (2019), Observations of potential meteors from asteroid 101955 Bennu, MNASSA 78, pp142-150.

Jenniskens, P., Lauretta, D., Koelbel, L., Towner, M., Bland, P., Heathcote, S., Abbott, T., Jehin, E., Hanke, T., Fahl, E., van Wyk, R., Cooper, T., Baggaley, J., Samuels, D., Gural, P., (2023), *An observing campaign to search for meteoroids of Bennu at Earth*, Icarus, 394, doi.org/10.1016/j.icarus.2022.115403.

Ye Q. (2019), *Prediction of Meteor Activities from (101955) Bennu*, Res. Notes AAS, 3, 56.

Znojil V. (1988), *Gnomonic Atlas Brno 2000.0*, WGN 16:4, pp 137-140.

Some thoughts on Dobsonian telescope bearings

Chris Stewart

A “Dobsonian” telescope is a Newtonian optical tube assembly mounted on a very simple but largely effective alt-az mount, typically made from plywood or particle board. This style of mount was popularised in the USA by one John Dobson, an eccentric sometime monk, who saw simplicity as a way to proliferate affordable telescopes. In this he was successful to the point that he has been immortalised through the adoption of his name for this style of telescope. Telescope manufacturers embraced the notion as a cost-cutting measure that could help boost sales, while the ranks of Amateur Telescope Makers swelled as the viability of producing a telescope without the need for expensive machining was recognised. This step-change in approach could rightfully be termed a revolution.

Unfortunately, there have also been some negative outcomes. Firstly, a lot of shoddily-built telescopes have flooded the market, and secondly many amateurs have slavishly followed earlier practices with a fervour that virtually makes them a cult.

Fortunately, there are also many amateurs (of which I am one) and some manufacturers who have been prepared to experiment, analyse and improve the art,

whilst still adhering to the basic concept. From these have arisen combinations of materials that work well together, notably the use of Teflon running against textured Ebony Star Formica – which the cultists laude as the pinnacle. Sadly for them, Ebony Star is no longer manufactured, which brings the Americans down to the same level as the rest of the world.

Some experimenters have reported success in introducing various lubricants, but these inevitably become contaminated, grow sticky as their volatiles evaporate, or are lost to the environment. Similarly, various other materials such as hard felt (perhaps impregnated with talcum powder) have been found to have their merits - and demerits. Of course, any working mechanism requires occasional maintenance to continue working effectively, and telescope bearings are no different. We would however prefer the maintenance to be simple and infrequent.

The first thing that one needs to understand is how such a telescope mount *should* behave - and then why it is *not* performing as desired. This ultimately boils down to friction, and its stepchild stiction.

Friction we generally understand intuitively – it is a resistance to movement between two parts that are in contact with one another. You have to apply a force to get a part in contact with another to move, and then you have to maintain the force to keep it moving. We make use of its benefits every day (you couldn't walk or keep a car on the road without it). But friction varies and, in some applications, too much is a bad thing as it increases wear and inhibits desired movement. Which is why bearings are a massive industry.

A prime consideration is the nature of the materials, especially as used in combination. Some have inherently high coefficients of friction, and such materials are good for making brakes. Others (like Teflon), which have a low coefficient of friction, are inherently slippery – but that often comes at a cost of being delicate, which reduces its lifespan.

Some material combinations have a low level of friction to start with, with the resistance climbing as the rate of movement increases. This is a generally desirable trait, at least to some extent. Others have a very high level of friction to start with, but once that is overcome, they suddenly move more easily – we call that stiction. In some applications, stiction has its uses, but in most cases (such as motorcycle forks or telescope bearings) it is highly undesirable. We see the effects of this when trying to track an object manually with our Dobsonian mounts. As the object drifts towards the edge of the field, we push to bring it back. Nothing happens for a moment, then suddenly the image jerks too far in the opposite direction. On motorcycle forks, it gives

a choppy ride that inhibits roadholding. For telescope users, it is not as dangerous but still very frustrating – and the effect is magnified as we move to higher-power eyepieces. Generally, stiction leads to a miserable experience.

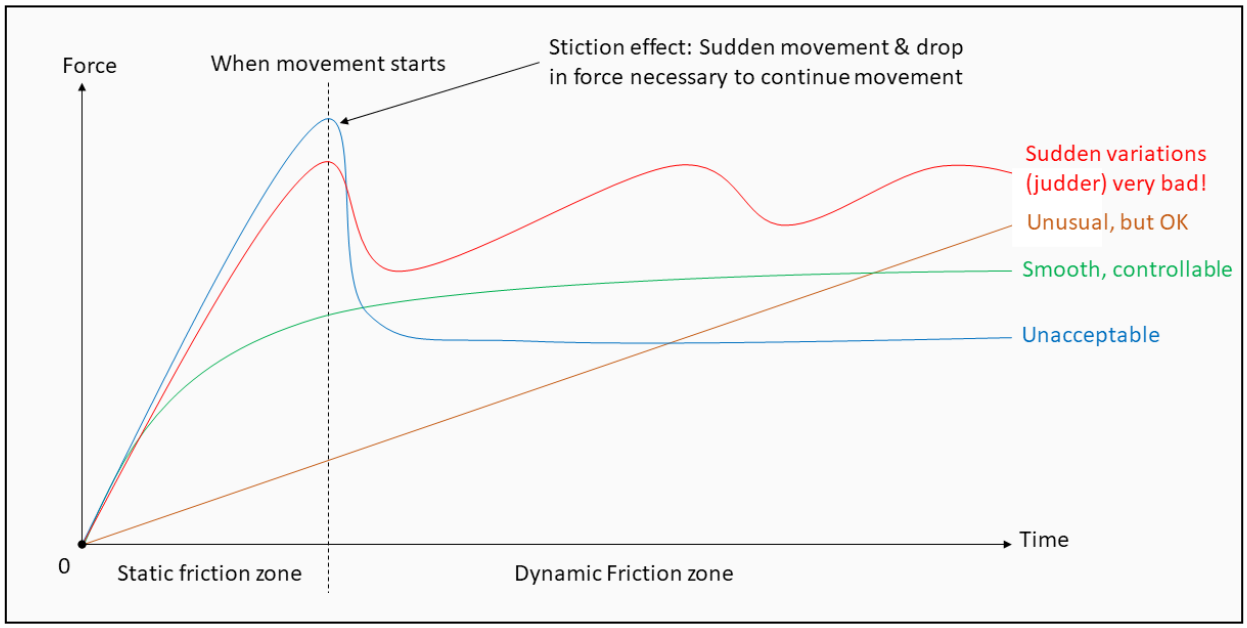

Fig 1. Friction effects on smoothness of movement.

One might therefore think that moving to ball bearings, which are designed to minimise friction, would be a good idea. And it does have its merits. However, too little friction can also be problematic. If your telescope is not 100% properly balanced in altitude, it will not maintain its position - the nose will either droop, or stand up under the force of gravity. If you have zero friction on your azimuth bearing, the slightest gust of wind will have the entire instrument spinning, and if it is not 100% level the scope will rotate "downhill". If you so much as brush your eyebrow against the eyepiece, you will lose the object. Either way, you will have to manage it continuously and there will always be visible vibration in the image. Again, a miserable experience.

It seems we are damned if we do, and damned if we don't. But there is hope. The key is to avoid extremes, and to manage both the amount and the nature of the friction, to keep things in the sweet spot. If one can separate the factors of supporting the load versus controlling the ease of movement, the battle is largely won.

The level of the problem is typically worse for the azimuth than the altitude bearing. One reason is that if (as is normal) you are pushing/pulling on the optical tube, the amount of leverage you have in azimuth varies according to the altitude. If the tube is horizontal the leverage is maximised, whereas if it is near the zenith it drops almost to zero. The altitude bearing does not have this variance (assuming the tube is properly balanced), as the distance from where you hold the tube to the axis - and thus the

leverage - remains the same. Also, the amount of friction involved varies with the load (the pressure forcing the materials into contact). This is higher for the azimuth bearing that must manage the weight of both the optical tube assembly and the rocker box structure, compared to the altitude bearing which need only handle the optical tube. Thus, if you are happy with the behaviour of the altitude bearing, you may wish to start with updating the azimuth bearing alone.

In this respect, it is useful to note that it is easier to add friction than to reduce it. From my experiments, *I strongly advocate using "proper" bearings, and then controllably adding friction to taste via a tuneable brake*. By "proper" I mean a bearing that will support the weight without inserting friction. This may seem complicated, but it is considerably easier than trying to go the other way. With imaginative sourcing of parts, it can be done quite inexpensively, and the reward is well worth the effort. You can even retrofit your existing scope fairly easily. Conceptually, it is quite simple. Put in ball bearings and a good surface for them to run against, then add a brake. [Of course, by putting in proper bearings, the design is strictly speaking no longer a Dobsonian, but that as a small price to play and only pedants like me are likely to quibble.]

Regarding the azimuth bearing you might find the "lazy-Susan" bearings intrinsically appealing. Those designed for rotating television stands or to allow people to access a tray of delicacies on the middle of a dining table certainly appear to be an attractive prospect. After all, they are readily available, relatively inexpensive, already have a central spindle, are rated for quite high thrust loads and have easy to use places to screw things together. NO! Please avoid these. Not being designed for our purpose where high magnifications demand excellent stability, they are not suitable: your telescope will rock every time you touch it. Although industrial needle-bearing lazy-Susans of larger diameter do exist and are an option, they are hard to find and very expensive. Far better is to add three ball bearings to the ground board, spaced as far from the central spindle as feasible, preferably directly over the feet that are in contact with the earth in order to transmit the load without distorting the bearing. These then run against a smooth plate affixed to the underside of the rocker box.

Metal on metal is fine, though it can be a bit rumbly and will eventually wear. You can mitigate this by choosing rubber coated bearings, though such things are hard to find at bearing suppliers. An easy answer is skateboard or roller-blade replacement wheels. They are designed to take much greater loads than your scope, and run at much higher rotation rates. One might imagine that after standing still for a while, the "tread" would develop a flat spot, but that has not been my experience.

For a very low-profile arrangement, you can substitute the ball/roller bearings with what are called "ball transfer units". These have a housing with a single large ball

protruding to support the load, backed up by a large number of smaller balls within the housing. The unit typically has a flange for mounting, which can if necessary be screwed down, whilst the body drops in to a pocket in the supporting plate. In use, the load can be moved in any direction in a plane, and it is perfectly adapted to take loads that travel in an arc. The downsides are somewhat higher pressure at the contact point, and a substantial increase in unit cost (but you only need three of them).

Unlike the brakes on a car, which are designed to quickly bring a large mass at high speed to a quick and complete stop, what I am referring to here is a friction pad that is in continuous contact, to prevent the axis from rotating too freely. My approach has been to use a lever or cam mechanism that applies pressure to the pad, but which is linked by a spring to a threaded rod. By screwing the rod, tension on the spring can be increased or decreased smoothly over a considerable range, thereby finely adjusting the pressure. This pad can run against the same plate as the bearing (which should of course be a smooth surface), but outside of the bearing track to avoid any roughness or scoring that might eventually arise after heavy use.

I have found HDPE (high-density polyethylene) to be an excellent material for this purpose. It is readily available worldwide. Thin portions (all one really needs) can be cut from scrap milk bottles and backed with a wood offcut to which they can be stapled. More “professional”, is to use thicker solid pieces. Obtaining a sheet from an industrial supplier is expensive when you really only need a small amount, but the same material can easily be cut from readily available catering cutting boards at a fraction of the price – and you will have a choice of colours. Teflon (aka PTFE, or polytetrafluoroethylene) is fine, but softer and considerably more expensive. Remember, whereas the traditional Dobsonian has a Teflon pad on which the full load rests, in this case we are only applying a fractional load to provide controllable drag.

The same procedure is also great for the altitude bearings. Attach a circular trunnion to each side of the optical tube assembly, just as you normally would for a Dobsonian, but instead of Teflon pads run it on roller bearings. Then, add a brake. I have found that a floating brake that pinches the trunnion between two pads works well. All you need to make sure of is that the pads remain stationary but accommodate any end-float of the trunnions.

For smaller scope, trunnions of Nylon, PVC or aluminium, with brake pads of Teflon or HDPE work well. Large industrial equipment wheels in Nylon, or large PVC pipes/fittings as a skin with a wooden core, are all very viable options. Plate bearings of glass (old CD / DVD) and HDPE are also smooth and cheap, being a workable size for such applications as binocular stands and small refractor mounts.

Don’t be afraid to experiment, and let us know your findings.

Case study 1: Argos Panoptes

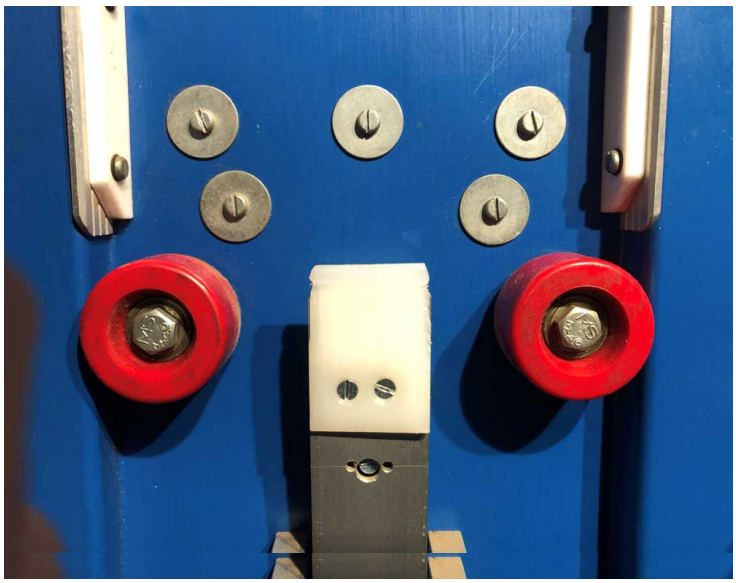

I built this 6” Newtonian in 1994 as a test bed for ideas, some of which are relevant here. This telescope has been heavily used, and despite its weight (having been built out of whatever scrap I could find) has been transported to distant lands over terrain so tough that rugged 4x4 vehicles broke. Despite this, it only needed a mirror cleaning and minor tweaking to realign the optics after 25 years. Relevant here are the following…

Fig 2. Rollers to support trunnion.

Trunnion on rollers. The altitude axis comprises two trunnions made from cast aluminium salvaged from the scrapyard. Each side rests on two rollers with ball-bearing centres, extricated from roller-skates. This takes the major load, but side-thrust is accommodated by the edge of the trunnion being constrained by the two vertical strips of salvaged white PTFE. Being held down by gravity, the only possible movement is rotation about the virtual altitude axis, as the trunnions roll on the roller-skate wheels. At the bottom, inboard from the trunnion, is the altitude brake. This comprises a flat vertical lever, which is hinged below (outside the photo) with the hinge pin horizontal and running left to right as viewed here. That constrains the free end “tongue” at the top to move towards or away from the trunnion, but not rock side to side. The white top end of the tongue is embedded in HDPE, so as to not mar the telescope tube on the visible side, and on the opposite hidden side to provide suitable friction against the flat inner edge of the trunnion. The blue part is the side wall of the mount rocker box.

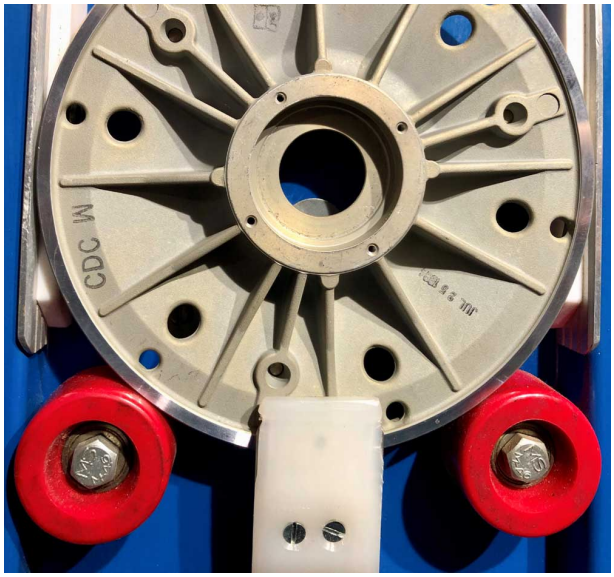

Fig 2a. Trunnion on rollers.

Note: Fig 2a shows the trunnion in place (separated from the telescope purely for this illustration), whereas Fig 2 shows the trunnion wheels and brake from the same perspective (but without the trunnion in place).

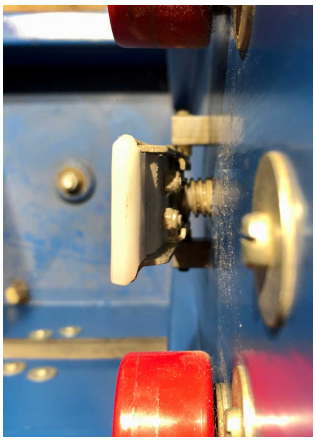

Fig 3. Altitude brake.

Altitude brake from top. Here you can see that the range of movement of the brake tongue is limited by a bolt passing through the blue side wall of the rocker box. Between the wall of the box and the tongue, surrounding the bolt, is a spring that biases the tongue inwards, away from the trunnion and towards the telescope tube.

Fig 4. More on altitude brake.

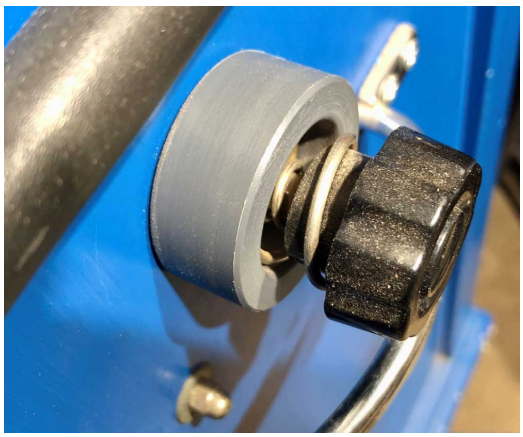

Outside the rocker box. The altitude brake bolt passes through an oversized hole in the rocker box and is surrounded outside by a stiffer spring that biases the brake tongue outwards, to pinch the trunnion against the PTFE strips. The balance of force between the two springs is adjusted by the knob on the end of the bolt. Tightening this, increases the drag on the trunnion rim, whereas relaxing it reduces the drag. This provides very precise control.

Fig 5. Azimuth brake.

Az brake overall. Here you are looking at two of the three legs of the base side-on, the third leg extending away into the background with only the rubber foot visible. Two of the ball bearings are visible, mounted on the trunnions salvaged from the roller skates used for the altitude axis. The ball bearing run directly against an aluminium disk. Stainless steel would have been better, but this is what I had. You can see that some dirt has been pressed into a track on the plate by the bearing outer cases, but despite the rumble you cannot see any image shake even at high power. The three bearings define the plane to which the plate aligns. A self-aligning bearing in the base of the rocker box engages a carriage bolt protruding upwards through the centre of the leg assembly, to define the azimuth axis. Its functions are to stop the rocker box from sliding horizontally, and to prevent the leg

assembly detaching. It takes little stress; the three vertical bearings take all the weight. Strung between the legs is the azimuth brake adjustment system. This comprises a threaded rod with a knob on the far right, which engages a nut in the white square tubing at centre, to which in turn is attached a braided stainless steel cable. The cable wraps around the pulley anchored to the screw hook at left and in turn attaches to the left end of a tension spring within the red plastic tube. The other end of the spring attaches to the L-shaped lever at centre. By rotating the knob, the screw draws the square tube to the right, pulling the cable, which then tensions the spring. The spring then applies force to the lever. The lever then transfers the force to the free end of a hinge, on the other side of which is a block of white HDPE that rides against the aluminium disk. Ultimately, rotating the knob adjusts the pressure of the HDPE against the plate, and thus the level of friction. This friction pad operates on the zone of the plate just inboard of the ball bearing track. Any dirt on the plate falls off, rather than becoming embedded in the HDPE. The hinge attached to the arm holding the friction pad, constrains movement of the pad to the vertical direction, as the hinge pin is tangential to the rotation of the rocker box. Again, the arrangement provides exquisite control of friction and seldom needs adjustment. Neither this nor the altitude brake have required maintenance during the lifetime of this scope.
In practice, they have proven to be a “fit and forget” arrangement. Once the sweet spot was quickly arrived at, the adjustment has since only been accessed to demonstrate the system.

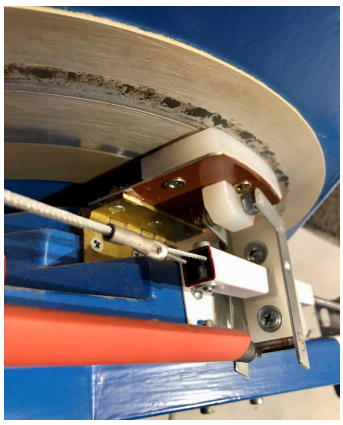

Fig 6. Azimuth brake closeup.

An alternate view from a different perspective. You can see that the square tube passes through a square hole in a block of HDPE, which allows it to slide linearly but not rotate.

Case Study 2 – Alternative Azimuth brake

Figs 7 & 8. Alternative Azimuth Brake.

This is a recent reprise of the brake detailed above, applied to a 5” scope. The principle is the same, but in the light of experience has been substantially simplified. Given that there is no need to access the adjustment knob frequently, the structure can be minimised and the entire

thing tucked away out of sight. One can however still reach under to access the knob. My fingers show that the size is much reduced. Again, the knob turns a screw that engages a nut, tensioning a spring, that through a lever presses upwards against the free leaf of a hinge, ultimately pressing a friction pad against the bottom of the rocker box, which has a smooth sheet of aluminium attached for both the brake and the azimuth bearings to run on.

Case study 3: Angel scope – a small refractor

Fig 9. Altitude trunnion bearings

Nylon pulleys with the edges machined flat, running on HDPE pads, make great altitude trunnions for a small scope. The outer edge of the pulley boss rubs against the wood, which is engineered bamboo (extremely hard resin-impregnated) to control end float. The movement is very smooth.

Fig 10. OTA at 45 deg

The azimuth bearing is a thin sheet of Teflon, sandwiched between two small hard disk platters. A spring around the upper portion of the azimuth spindle bolt which (the end of which can just be seen poking up), presses down on the central bearing to provide pressure on the sandwich. Again, the movement is very smooth.

Case Study 3 – Julian Shellard's trio of scopes

Fig 11. Julian-scopes

Here you can see a common thread. In each of these scopes the altitude trunnions are PVC, running against the edges of two dowels of Nylon. These too have very smooth actions. The one closest in this photo has an interesting twist: the two altitude trunnions are different sizes. By adopting this approach, two advantages accrue. Firstly, it is easier to tune the friction. Secondly, the arrangement creates a virtual cone that more tightly defines the altitude axis - this prevents the trunnions from riding out of their sockets when lateral force is applied to move the scopes in azimuth.

Darkness and colour of the Total Lunar Eclipses of 2022

Tim Cooper, Bredell Observatory

Summary
It has long been known that dark lunar eclipses follow shortly after major volcanic eruptions. Observations of darkness and colour of lunar eclipses can be used to determine the visual magnitude of the eclipsed Moon, which is related to conditions in the Earth's atmosphere at the time of eclipse.

The most recent significant volcanic eruption was that of Hunga Tonga-Hunga Ha'apai in January 2022, and thus it was of interest to see what the effect would be of the eruption on the darkness and colour of the two Total Lunar Eclipses on 16 May and 8 November 2022. Observations are presented for the first eclipse, which indicate that, while the eruption did affect the Moon's brightness during eclipse, the degree to which the Moon was darkened was probably less than expected following on from a major volcanic eruption.

Note: All times referred to are in UT.

Darkness of lunar eclipses and volcanic activity
During a lunar eclipse, the Moon passes through the shadow of the Earth cast in space. In theory the portion of the Moon within the umbral shadow should be black and disappear, but in practice the eclipsed Moon usually remains visible and is coloured. This is a result of refraction of sunlight by the Earth's atmosphere, and depends on conditions within the portions of atmosphere through which sunlight passes at time of eclipse. A discussion of factors affecting the darkness and colour of lunar eclipses can be found in Cooper (2004) and Cooper and Jacobs (2018), and a summary will suffice here. Sunlight is scattered due to interaction with particles in the atmosphere. Scattering by very small particles (Rayleigh scatter) is inversely proportional to the fourth power of the wavelength, with the result that blue light is scattered more than red light, which preferentially passes through and results in a more red eclipse. In cases where the scattering particles are more or less the same size (Mie scatter) or larger than the wavelengths of visible light (non-selective scatter), sunlight is attenuated, resulting in a darker eclipse. In addition, several molecular species normally present in the atmosphere, including ozone and water vapour, as well as atmospheric pollutants, including nitrogen oxides and sulphur dioxide, absorb sunlight in specific visible wavelength bands, so that the transmitted light is deficient in those wavelengths, and the colour of light incident on the Moon's surface is altered. One major factor affecting the darkness and colour of lunar eclipses is the presence of solid particles and gaseous molecules injected into the upper atmosphere during volcanic activity. Flammarion

was the first to point out that dark lunar eclipses followed volcanic eruptions, after the eruption of Krakatau in 1883 (Stothers 2004). Danjon (1920) introduced a five point scale to characterise colour and luminosity of the eclipsed Moon (Table 1):

Danjon L value	Description
0	Very dark eclipse, moon almost invisible, especially in mid totality
1	Dark eclipse, grey or brownish colouration; details distinguishable only with difficulty
2	Deep red or rust coloured eclipse, with a very dark central part in the umbra and the outer rim of the umbra relatively bright
3	Brick red eclipse, usually with a bright or yellow rim to the umbra
4	Very bright copper red or orange eclipse, with a bluish, very bright umbral rim

Table 1. Danjon Luminosity scale for lunar eclipses

Danjon applied his scale to seventy lunar eclipses between 1823 and 1920, and concluded there was a relationship between eclipse darkness and the 11-year solar cycle, with darker lunar eclipses coinciding with solar maximum. Link (1974) in a discussion of lunar eclipse observations since 1900 'confirmed the validity of Danjon's law describing the variations of the luminosity of lunar eclipses during the solar cycle of 11 years'. However, neither Danjon nor Link made any mention of the effect of volcanic eruptions on eclipse darkness.

Keen (1983) used lunar eclipse observations to determine optical depth of the atmosphere, and concluded that such observations provide an instantaneous measure of globally averaged aerosol absorption. When plotting optical depth against date of eclipse, and superimposing dates of volcanic activity, there is compelling evidence for the effect of the latter on lunar eclipse darkness, see Figure 1.

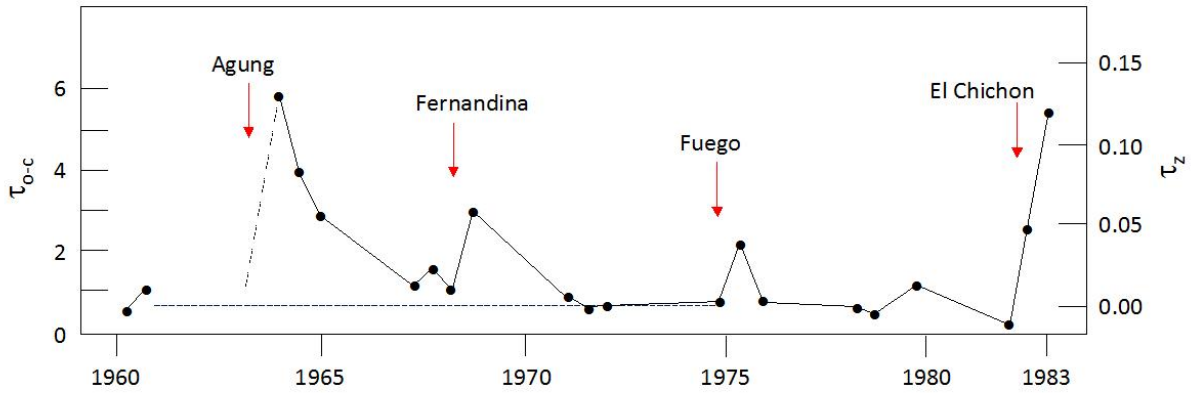

Fig 1. Plot of atmospheric optical depth with date, adapted from Keen (1983). Black dots are optical depths derived from lunar eclipse observations. Eruption dates are shown for four volcanoes: Agung March 1963 (VEI 5), Fernandina June 1968 (VEI 4), Fuego October 1974 (VEI 4) and El Chichón March 1982 (VEI 5).

Keen (2016) also showed that aerosols injected into the atmosphere can take several years to decay, leading to elevated optical depths and darker eclipses which may persist for some time after an eruption.

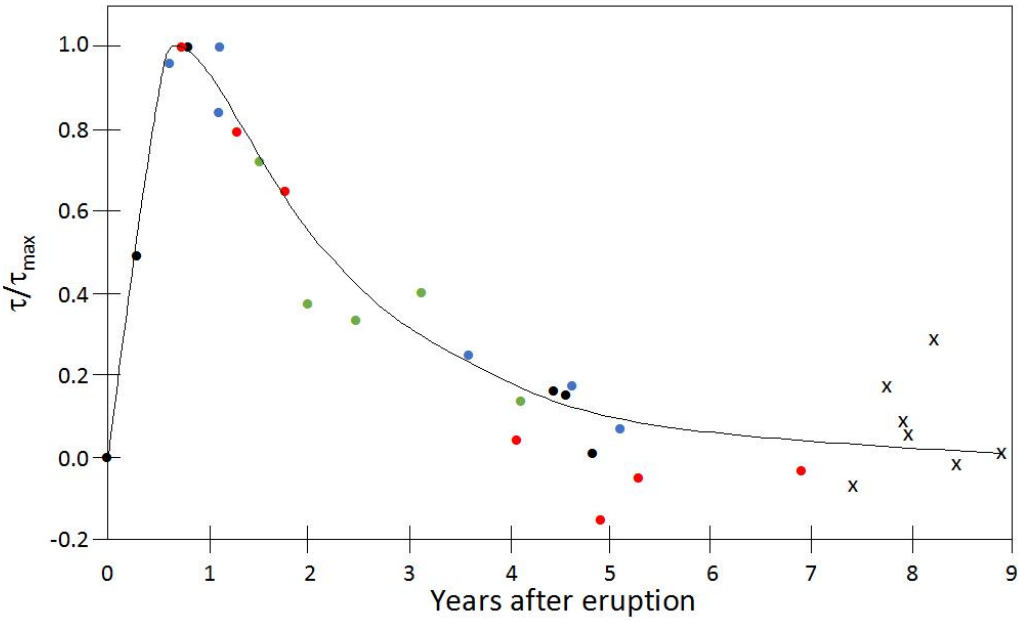

Fig 2. Decay in atmospheric optical thickness as a fraction of the peak value for four volcanoes derived from lunar eclipse observations. Black dots = El Chichón, blue dots = Krakatau, red dots = Agung, green dots = Pinatubo, x are unidentified. Data from Keen (2016).

Figure 2 shows the measured optical depth (τ) as a fraction of the maximum optical depth (τ_{max}) for the four large volcanic eruptions in Table 2 and derived from observations of lunar eclipses immediately following those eruptions. The rise to maximum optical depth can take several months, though the actual slope of the rise in

Figure 2 is based on only one eclipse measurement which followed 176 days after the eruption of El Chichon in 1982, and is therefore uncertain. However, in most cases maximum optical depth was reached within 12 months following large eruptions. Thereafter there is a slow decay in volcanic aerosols, which may take several years, during which period the darkness of lunar eclipses may be affected.

Volcano	**Location**	**Lat °**	**Long °**	**Date**	**VEI[1]**	**Next TLE**	**Days**	**UM[2]**
Krakatau	Indonesia	6.10 S	105.42 E	27/8/1883	6	4 10 1884	404	1.53
Agung	Indonesia	8.34 S	115.50 E	17/3/1963	5	30 12 1963	188	1.34
El Chichón	Mexico	17.36 N	93.23 W	29/3/1982	5	30 12 1982	176	1.18
Pinatubo	Philippines	15.14 N	120.35 E	15/6/1991	6	9 12 1992	543	1.27

Table 2. Details for eruptions of volcanoes shown in Figure 2. Data from Smithsonian Institution, National Museum of Natural History, Global Volcanism Program at https://volcano.si.edu/.

Notes to Table 2:

Note 1 : VEI = Volcanic Explosivity Index, is a logarithmic scale that describes the volume of ejecta and column height of volcanic eruptions. The scale runs from 0 to 8, with values of 5 to 8 representing ejecta volumes of 10 km^3, 100 km^3, 1000 km^3 and > 1000 km^3 respectively.

Ref: https://www.nps.gov/subjects/volcanoes/volcanic-explosivity-index.

Note 2 : UM = Umbral Magnitude of eclipse, is the depth of immersion of the Moon expressed as a fraction of the Moon's disk inside Earth's umbral shadow. If UM is in the range 0 to 1 the eclipse is partial, and the eclipse is total for all values UM>1. Note Umbral Magnitude UM of the eclipse should not be confused with the visual magnitude (m_v) of the eclipsed Moon, and are two distinctly different parameters. The value of UM is fixed for any one eclipse, while the value of m_v varies from eclipse to eclipse and needs to be measured.

Di Giovanni (2018) extended the analysis to 164 lunar eclipses occurring between 1670 and 2015, and found a correlation of eclipse darkness with both volcanic and human activity, but no correlation with solar activity.

Methodology

The darkness of lunar eclipses can be measured by amateur astronomers using several fairly straightforward techniques. Keen (1986) showed that Danjon luminosity values can be used to determine the visual magnitude of the Moon during eclipse using the formula:

$$m_v = 3.99 - 3.13L + 0.364L^2 \qquad (1)$$

where L is the observed Danjon luminosity value derived from observations using the scale in Table 1. The estimate is made with either the naked eye or instrument with small aperture and magnification, such as a pair of binoculars, and is a simple and convenient way of ranking the darkness during totality. The degree to which different colours are seen in the eclipsed Moon forms an important part of the observation. The magnitude of the Moon can also be determined using Selivanov's reverse binocular method (see for example Sinnott 1975), which relies on the principle of looking through the objective end of a pair of binoculars with one eye in order to diminish the Moon's brightness and comparing the brightness of the reduced image with stars and planets as seen with the unaided eye. The method is analogous to Argelander's method for estimating brightness of variable stars. The visual magnitude of the eclipsed Moon can then be determined using the formula (Keen 1986):

$$m_v = RB - (0.2 + 5\log M_B) \qquad (2)$$

where RB is the estimated reversed binocular magnitude and M_B is the magnification of the binoculars. The estimates can be made throughout the eclipse, starting before first contact of the umbra (U1), more frequently during totality (between U2 to U3) and continuing until after last contact of the umbra (U4), depending on the visibility of the eclipse from the observing site. The estimates can then be used to construct a light curve in order to determine the integrated brightness of the Moon as the eclipse progresses, as well as at the moment of mid-eclipse.

More recently Di Giovanni (2018) has developed procedures to determine pixel values from digital images of the Moon taken before and during eclipse. From these measurements, isophote mapping of lunar brightness can be made in the three colour channels (RGB), which give more information on inhomogeneity in the atmosphere as the eclipse progresses. The optical depth can be further derived from the integrated lunar luminosity at time of maximum eclipse. ASSA has participated in these studies since the 27 July 2018 TLE.

The eruption of Hunga Tonga-Hunga Ha'apai (HTHH) in 2022

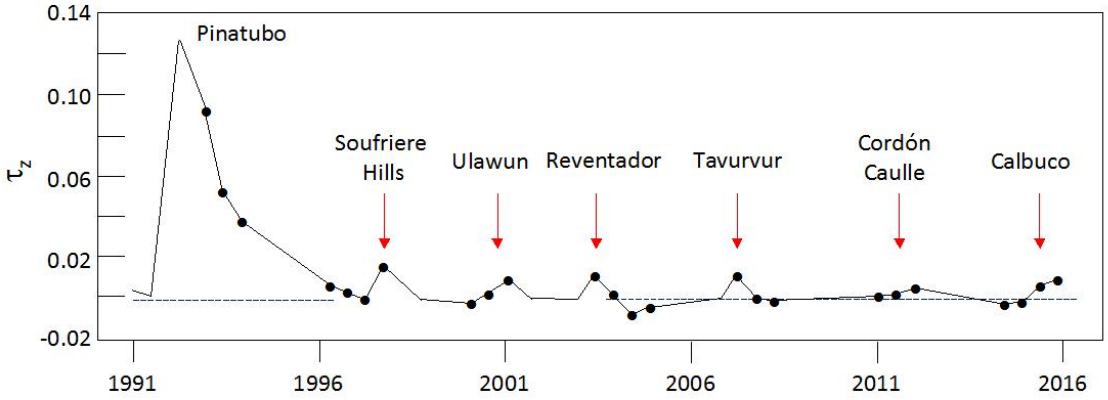

Fig 3. Atmospheric optical thickness measured from lunar eclipse observations since Pinatubo eruption in 1991. Adapted from Keen 2016.

The optical depth of the atmosphere (τ_z) has been relatively low since the decay in atmospheric aerosols following the eruption of Pinatubo in 1991 (Figure 3), which resulted in a very dark eclipse (L=0, UM=1.27, see O'Meara 1993) on 9 December 1992, 543 days after its VEI 6 eruption on 15 June 1991. There have been no VEI 6 eruptions since Pinatubo, and although a VEI 5 eruption occurred from Puyehue-Cordón Caulle starting on 4 June 2011 [Data from Global Volcanism Program - Volcanoes of the World 5.0.0, downloaded on 18 Nov 2022 from https://volcano.si.edu/] the lunar eclipse which followed 189 days later on 10 December 2011 remained fairly bright (L=3.2). HTHH has erupted on several occasions since 1912, mostly with VEI $\leq$ 2. The present activity commenced on 20 December 2021, then escalated on 14 January 2022, before undergoing a major eruption on 15 January 2022 (VEI 5), the most explosive since Pinatubo in 1991. The eruption occurred from below sea level. Yuen et al (2022) called it 'arguably the most violent volcanic eruption in the past 138 years'. The explosion injected ash into the mesosphere at an altitude of 58km (Figure 4, Bates and Carlowicz 2022), the tallest volcanic ash cloud ever recorded in satellite data.

The initial cloud expanded to diameter 500 km (NASA 2022), and thereafter was dissipated downwind, increasing in area to 1.2 x 10^7 km^2 by 19 January (Terry et al, 2022), and reaching East Africa by 22 January (GVP 2022). Cronin says (2022) the eruption of HTHH was the largest ever recorded, and a remarkable feature was the speed at which the plume expanded. However, despite the size of the eruption, it did not produce large amounts of sulphur dioxide (SO_2), only around 450 kt combined for the earlier smaller eruptions and the large eruption on 15 January 2022, or around 2% of the SO_2 emitted by Pinatubo. Nevertheless, as with Pinatubo, gases emitted by HTHH produced vividly coloured sunsets, as evidenced by images taken by Angus Burns (Figure 5).

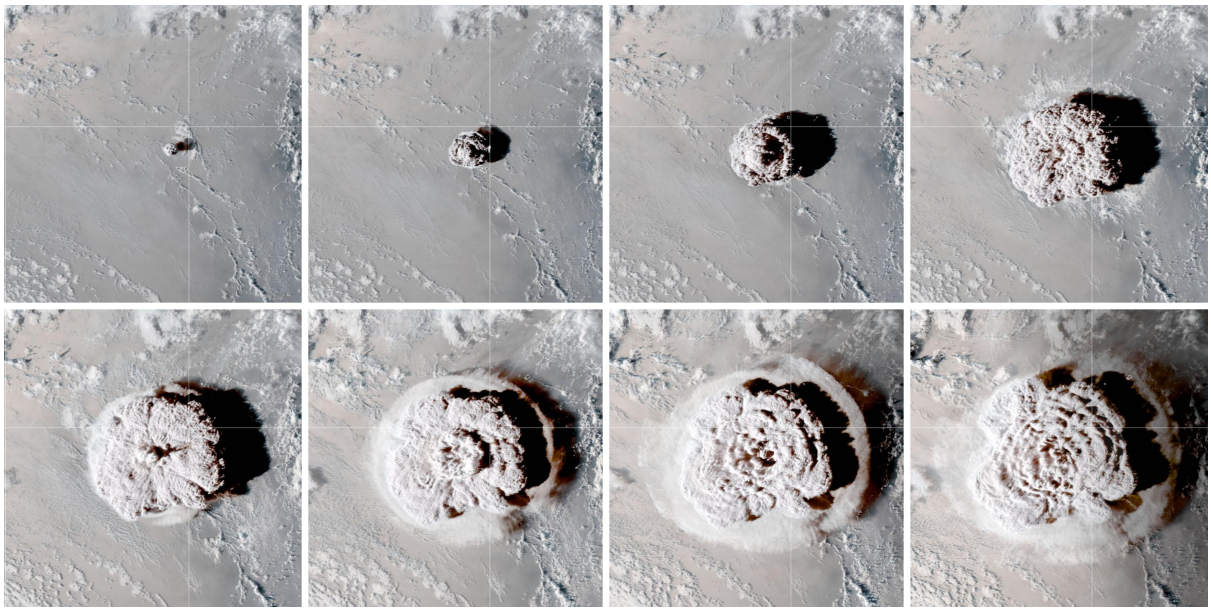

Fig 4. Sequence of images of eruption of HHTH on 15 January 2022, starting upper left at 04h10 UTC, to lower right at 05h20 UTC. From measurement of shadow lengths the plume was ascertained to reach an altitude of 58 km, extending into Earth's mesosphere. NASA Earth Observatory images and by Joshua Stevens, using data courtesy of Kristopher Bedka and Konstantin Khlopenkov/NASA Langley Research Center, and GOES-17 imagery courtesy of NOAA and the National Environmental Satellite, Data, and Information Service (NESDIS).

Fig 5. Images of brightly coloured sunsets by Angus Burns, Newcastle, KZN, following the eruption of HTHH on 15 January 2022. Left image taken on 22 February 2022, Canon 5D Mark IV, 24-70mm F4L IS USM lens, ISO800, f/4.5, 1/15 second exposure. Right image taken on 16 June 2022, Canon 5D Mark IV, 24-70mm F4L IS USM lens, ISO400, f/4, 1/30 second exposure. Both images unprocessed.

O'Meara (2022) observed 'five days later, the cloud passed over southern Africa' and 'contrast between the clouds and sky intensified around the time of sunset, when they underwent magnificent colour changes, morphing from silvery blue to tangerine infused with lemon to a velvety scarlet'. Given the size of the eruptions, the rapid expansion of the ash cloud, and the presence of gases which produced exaggerated coloured sunsets, it might be expected that the eruption of HTHH would have an effect on darkness and colour of the lunar eclipses on 16 May and 8 November 2022.

Observations of the 16 May 2022 Total Lunar Eclipse, UM = 1.41

The TLE of 16 May 2022 followed the eruption of HTHH by 121 days. Considering the time to reach peak optical depth in Figure 2, this is a rather short period compared to other major eruptions, and despite the fact ejecta from HTHH spread rapidly, this period is possibly too short to have had a major influence on darkness of the eclipse. On the other hand the eclipse was quite deeply immersed in the umbra, with UM = 1.41, and the Moon passed through the parts of the atmosphere south of Earth's equator, the zenith latitude at mid-eclipse being -19.3° (Espenak 2023), very close to the -20.6° latitude of HTHH. Also, since the HTHH plume extended to an altitude of 58 km, and spread rapidly by prevailing winds it might be expected the increase in atmospheric optical depth in the case of HTHH would proceed in a shorter period compared to the four eclipses in Figure 2.

Circumstances of the eclipse are given in Table 3. Unlike the previous TLE visible from southern Africa on 27 July 2018, circumstances were less favourable for observation, with maximum eclipse occurring at 04h11, Moonset for Johannesburg at 04h29, end of total eclipse at 04h54, and Moonset for Cape Town at 05h20. Therefore observers in Gauteng would see maximum eclipse with the Moon at lower altitude. The effect of observing at low altitude is for the Moon to be redder and fainter than would otherwise be the case if it were higher in the sky. Consequently observers in the Western Cape witnessed maximum eclipse with the Moon at higher elevation above the horizon, and this fact should be born in mind in when comparing observations made from Gauteng and the Western Cape.

<u>Visual colour descriptions</u>

The author conducted visual observations of the Moon during eclipse. These descriptions were compared to the descriptions in the Danjon scale to estimate Luminosity (L) values.

Event	Contact	Contact Time UT1	Altitude of moon Johannesburg °	Altitude of moon Cape Town °
Penumbral Begins	P1	01:31:43.9	39.5	47.5
Partial Begins	U1	02:27:30.8	27.6	36.3
Total Begins	U2	03:28:39.5	14.4	24.3
Greatest Eclipse	UM = 1.41	04:11:31.2	5.8	16.0
Moonset Johannesburg		04:29		
Total Ends	U3	04:54:11.5	Below horizon	7.8
Moonset Cape Town		05h20		

Table 3 Circumstances for the 16 May 2022 TLE

02h50, 16x50 binoculars, umbra distinct copper colour.
03h09, naked eye, umbra perceptible copper-orange.
03h32, naked eye, outer umbra pale yellow, inner umbra dull copper-orange. L=3.
03h35, smoky grey patch in NW quadrant, including Mare Imbrium and N Oceanus Procellarum, surrounded by dull smoky orange band, including Mare Frigoris, Serenitatis, Nubium and S Oceanus Procellarum, pale yellow crescent from W limb, through S and E limbs to N limb, bright in SE. L=3 (Figure 6 left).

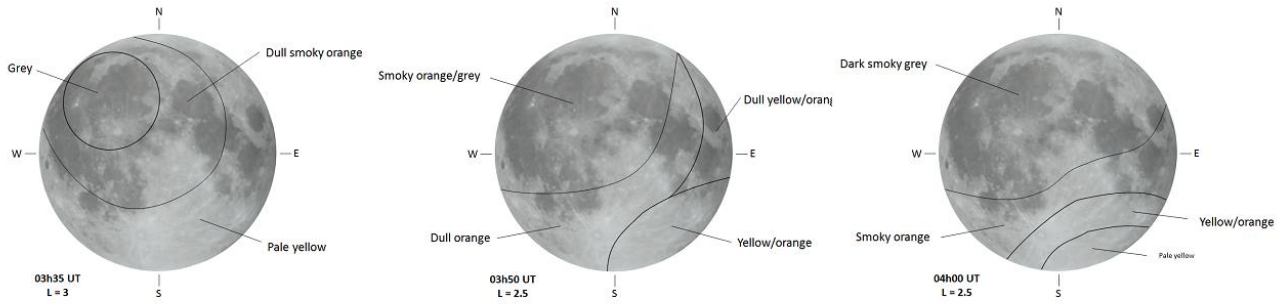

Fig 6. Visual observations of colour by the author. Note directions are in selenographic coordinates. Observations made using 16x50 binoculars.

03h50, looking west with Moon at low altitude, left hand side (S and E quadrants) bright yellow-orange, NW hemisphere dark rust or smoky orange, grey central shadow, SW limb dull orange crossing to NE limb which is dull yellow orange. L=2.5 (Figure 6 centre). **04h00**, definite yellow colour at S limb, inner shadow dark smoky grey, moon is more orange or brick red than dark red, therefore L=2.5 (Figure 6 right). But twilight now becoming bright and clouds approaching Moon from above and moving towards west. Carol Botha imaged the eclipse from Gordon's Bay, and her image taken close to mid-totality (Figure 7) is a good representation of the visual appearance as described by the author.

Fig 7. Image of the 16 May 2022 Total Lunar Eclipse taken by Carol Botha from Gordon's Bay, near mid-eclipse, Canon 5D MkII on tripod, Canon EF 400mm lens at f/5.6, exposure time 1.3 seconds at ISO 640. Image reoriented to give selenographic North above, and East right. Compare image with colour descriptions in the right-hand sketch by the author in Figure 6.

Estimates of eclipse darkness

Based on visual observations and the foregoing descriptions the author estimated Danjon luminosity L=2.5 at 04h00, shortly before mid-eclipse, but the altitude of the Moon was only 8° at that time. As with the 2018 TLE, the author again requested estimates of Danjon values on the Sterre en Planete Facebook page. Estimates were provided by eleven individuals as follows: Petrus Pienaar (Boksburg), Wessel du Preez (Vrede), Stephanus du Toit (Deneysville), Willem Morton (Namibia), and Pieter Swanevelder, Bell Clayton, Fuad Allie, Erna Gerber, Johan le Roux, Willem le Roux and Gary Deacon (all Western Cape). Angus Burns and Lafras Smit reported cloud from Newcastle and between Heilbron and Frankfort respectively. These estimates, when combined with the author's, gave a mean L = 2.0. The mean values for observers based in Gauteng and Free State, and for the Western Cape and Namibia, where the altitude of the Moon was higher at mid-eclipse, both averaged L = 2.0, but the results have high degree of scatter due to the small sample size. Elsewhere, other experienced collaborators estimated lunar brightness. In Brazil, Willian Souza estimated L = 2, as did Bob Lunsford in California. Giovanni Di Giovanni estimated L = 2 to 2.5 from Italy, where the Moon was also at low altitude. Taking the mean of all observations as L = 2.25 ± 0.25, without correcting for atmospheric extinction, and using equation 1, the visual magnitude of the Moon at mid-eclipse was $m_v = -1.24 \pm 0.4$.

Apart from Danjon estimates the author produced reversed binocular estimates using 16x50 binoculars, starting at 02h15, and up to 03h45, when the moon became too faint to be detected. At that time however the Moon's altitude was only 11°. Using equation (2) and correcting for atmospheric extinction using Appendix E of the Handbook for Observing Comets issued by the ICQ, the brightness of the Moon at 03h45 was fainter than magnitude -3.2. No further conclusion can be made. Using images of the eclipse provided by Kos Coronaios, Di Giovanni (2022a) determined the magnitude at mid-eclipse as m_v = -1.0, and commented that this measurement indicates the Moon was darker than the previous TLE on 27 July 2018. From the mean Danjon value for the 16 May TLE, he further determined an optical depth of 0.07, higher than the eclipse of 27 July 2018 which was near to zero (Di Giovanni 2022b).

The 8 November 2022 Total Lunar Eclipse, UM = 1.36

Unfortunately the second TLE of 2022 was not visible from Southern Africa. Nevertheless, two associates Rikki and Krish Lamba observing from Cleveland, Ohio, managed to image the eclipse at various stages, including the image at mid-eclipse shown in Figure 8.

Figure 8 Image of the 8 November 2022 Total Lunar Eclipse by Rikki and Krish Lamba. Image taken at 11h01 UT, Canon EOS 7D, APS-C DSLR, Tamron SP 150-600mm set at 600mm, f/6.3, 1.3 seconds exposure at ISO 1600. Note mainly brick-red or rust colouration, but outer umbra relatively bright, consistent with their Danjon L=2 rating.

At the same time they agreed on a Danjon estimate of L=2. The altitude of the Moon at the time was 12°, and so the measurement is comparable with observations of the 16 May eclipse made from Southern Africa where the Moon was at similar altitude. Their image showing more brick-red colouration than orange, and the Danjon value indicate the Moon during the 8 November TLE was certainly not brighter than the 16 May TLE.

Discussion

The various estimates of eclipse darkness from the last three Total Lunar Eclipses are summarised in Table 4.

Eclipse	UM	m_v instrumental	m_v Danjon	tau
27 July 2018	1.61	-1.25 ± 0.25	-1.7	~ 0
16 May 2022	1.41	-1.0 ± 0.25	-1.24 ± 0.4	0.07
8 November 2022	1.36	Not determined	-0.8	Not determined

Table 4 Comparison of brightness measurements, last three Total Lunar Eclipses. The 2018 TLE was pre-eruption of HTHH, the two 2022 TLEs were 121 and 297 days after HTHH respectively. UM is the Umbral Magnitude of the eclipse, tau is the optical depth of the atmosphere derived by Di Giovanni (2022b).

The brightness of the eclipsed moon derived from instrumental methods is seen to be slightly darker than that derived from Danjon estimates, but both confirm the 16 May 2022 TLE, which occurred after the eruption of HTHH, was darker than the 27 July 2018 TLE which occurred several years prior to the eruption. The decreased brightness of the Moon during the 16 May 2022 TLE is despite the fact the Moon was less immersed in the Earth's umbral shadow; the 27 July 2018 TLE had L = 2.62, described as considerable orange colouration rather than deep red or brown, with a bright yellow edge to the umbral shadow, consistent with a brighter eclipse, while the 16 May 2022 TLE had L = 2.25, described as definite yellow colour at the Moon's Southern limb, inner shadow dark smoky grey, Moon more orange or brick red than dark red. However, the estimated L value of the 16 May eclipse indicates the eclipse was probably not as dark as might be expected following a major volcanic eruption, though the eclipse occurred only 121 days after eruption and the atmospheric optical depth had not yet had time to reach its peak value. The 8 November eclipse was not visible from Southern Africa, but from the few measurements obtained elsewhere, the Moon was possibly slightly darker than the 16 May eclipse.

Next Total Lunar eclipses

The next TLE occurs on 14 March 2025 but is not favourable for observation from Southern Africa. The next favourable TLE for the region occurs on 7 September 2025 with UM = 1.36, and mid-eclipse at 18h13, when the Moon will be 30° above the horizon at Johannesburg. This is followed by a UM = 1.25 TLE on New Year's Eve, 31 December, 2028 with mid eclipse occurring at 16h53, but the Moon will be below the horizon at that time. It rises in bright twilight still totally eclipsed, and end of umbral eclipse occurs at 18h36 when the Moon will be 17° above the horizon at Johannesburg. In 2029 we get to enjoy a bumper year for Total Lunar Eclipses; the first occurs on 26

June 2029, and with UM = 1.84, the Moon will pass almost through the centre of Earth's umbral shadow. The last TLE of the decade occurs on 20/21 December, when mid eclipse is at 22h43 with UM = 1.12, and the entire eclipse is visible from Southern Africa.

Conclusions

Both instrumental and visual observations confirm the TLE of 16 May 2022, which occurred 121 days after the VEI 5 eruption of HTHH, was darker than the previous TLE on 27 July 2018 which occurred before the eruption. Optical depth increased from near zero to 0.07. The eclipse was less dark than those following previous major eruptions, including most recently the VEI 6 eruption of Pinatubo in 1991. The few images and a single Danjon estimate indicate the 8 November 2022 TLE was not brighter than the 16 May 2022 TLE, but possibly slightly fainter indicating the optical depth as a result of the HTHH eruption had not yet peaked. Once again a call is made for more individuals to get involved in making these measurements. They are ideally suited for observation with the naked eye or binoculars and do not require years of experience, rather an aptitude to carefully record what the eye sees, and provide the opportunity to make a scientific observation of one of nature's most beautiful phenomena.

References

Bates, S. and Carlowicz, M. (2022).
https://earthobservatory.nasa.gov/images/149474/tonga-volcano-plume-reached-the-mesosphere

Cooper, T. P., (2004), *The darkness and colour of the umbra during a lunar eclipse*, *MNASSA* **63,** pp60-64.

Cooper, T. P. and Jacobs, P., (2018), *Observations of the darkness and colour of the 2018 July 27 Total Lunar Eclipse*, *MNASSA* **77***, pp179-200.*

Cronin, S., Kula, T., Brenna, M., Ukstins, I., Adams, D., White, J., Paredes, J., Baxter, R., Wu, J., Kilgour, G., Barker, S. and Hamilton, K., (2022), *Insights into a large explosive eruption – Hunga Volcano, Tonga*, from a talk on YouTube, https://www.youtube.com/watch?v=4N2U8h92OPI.

Danjon, A. (1920), *On a relationship between the illumination of the eclipsed moon and solar activity*, *Compt. Rend*. **171**, p1127, and *New determination of the solar period based on the law of illumination of lunar eclipses*, ibid p1207.

Di Giovanni, G., (2018), *Lunar eclipse brightness and the terrestrial atmosphere*, *JBAA*, **128,** pp10-17.

Di Giovanni, G., (2022a), private communication dated 27 May 2022.

Di Giovanni, G., (2022b), private communication dated 26 June 2022.

Espenak,F., (2023), Total Lunar Eclipse of 2022 May 16, at Eclipsewise.com, https://www.eclipsewise.com/lunar/LEprime/2001-2100/LE2022May16Tprime.html

GVP, 2022, Report on Hunga Tonga-Hunga Ha'apai (Tonga), Weekly volcanic activity report, 19 Jan–25 Jan 2022, Sennert, S.K. (ed.), Global volcanism program, Smithsonian Institution and US Geological Survey https://volcano.si.edu/showreport.cfm? doi= GVP. WVAR2 022b0 119- 243040. Accessed Jan 2022.

Keen, R. A., (1983), *Volcanic Aerosols and Lunar Eclipses*, *Science,* **222**, pp1011-1013

Keen, R. A., (1986), private communication dated 18 September 1986.

Keen, R. A., (2016), *Volcanoes and climate change since 1980; a view from the moon*, slides downloaded from https://slideplayer.com/slide/16954099/, presentation by Richard A. Keen, Atmospheric and Oceanic Sciences, University of Colorado, Boulder.

Link, F. (1974), *Some remarks on Danjon's Law, The Moon*, **11,** pp137-140

NASA, 2022, Tonga Volcanic Eruption & Tsunami, National Aeronautics and Space Administration. https://appliedsciences.nasa.gov/what-wedo/disasters/disasters-activations/tonga-volcanic-eruption-tsunami. Accessed April 2022.

O'Meara, S. J., (1993), The Night the Moon Disappeared, in *Sky and Telescope*, **85**, April 1993, p107.

O'Meara, S. J., (2022), *Volcanic twilights*, in *Astronomy* magazine, August 22 issue, published 1 August 2022.

Sinnott R. W., (1975), *An Observers Kit for This Month's Lunar Eclipse*, *Sky and Telescope*, **49**, No. 5 (May 1975) pp280-283.

Stothers, R. B., (2004), *Stratospheric transparency derived from Total Lunar Eclipse Colors, 1665-1800, Publ. Astron. Soc. Pac.* **116,** pp886-893.

Terry, J. P., Goff, J., Winspear, N., Bongolan, V. P. and Fisher, S., (2022), *Tonga volcanic eruption and tsunami, January 2022: globally the most significant opportunity to observe an explosive and tsunamigenic submarine eruption since AD 1883 Krakatau*,

Geoscience Letters 9:24, downloaded from https://doi.org/10.1186/s40562-022-00232-z

Yuen, D. A., Scruggs, M. A., Spera, F. J., Zheng, Y., Hu, H., McNutt, S. R., Thompson, G., Mandli, K., Keller, B. R., Wei, S. S., Peng, Z., Zhou, Z., Mulargia, F. and Tanioka, Y., *Under the surface: Pressure-induced planetary-scale waves, volcanic lightning, and gaseous clouds caused by the submarine eruption of Hunga Tonga-Hunga Ha'apai volcano*, Earthquake Research Advances 2 (2022) 100134, https://doi.org/10.1016/j.eqrea.2022.100134.

Colloquia

Colloquia and Seminars (now Webinars) form an important part of a research facility, often as a sort of pre-publication discussion or a discussion of an individual's current research, and as such it is virtually impossible to "publish" this material. However by recording the topics discussed in the form below does indicate to those, who are unable to attend, what current trends are and who has visited to do research: it keeps everyone 'in the loop' so to speak

These form an important part of a research facility, often as a sort of pre-publication discussion or a discussion of an individual's current research, and as such it is virtually impossible to "publish" this material. However, by recording the topics discussed in the form below does indicate to those, who are unable to attend, what current trends are and who has visited to do research: it keeps everyone 'in the loop' so to speak

With the advent of CV19, these Colloquia and Seminars are being presented to wider audiences via Zoom and other virtual platforms. The editor has started by identifying what would originally been "local" Colloquia and Seminars; not easy as there are now Webinars on interesting topics from around the globe! In time we will either return to the traditional Colloquia and Seminars or many will become Hybrid session.

Title: How to take direct images of Exoplanets?
Speaker: Dr. Garima Singh
Date: 26 January
Venue: SAAO – Venue: Online SAAO Zoom
Time: 09h00

Abstract: Exoplanets are planets that orbit stars other than the Sun. As of today, more than 5000 exoplanets have been discovered in our Milky Way galaxy alone. NASA's statistics state that each of the 300 billion stars in our galaxy has at least one planet orbiting it. Such exoplanet discoveries are already helping us to understand how

planets form and evolve and what the atmospheres of exo-worlds look like, however, finding signs of life outside of Earth is still an unachievable feat.

One way to find exoplanets is the direct imaging method, which translates into taking family portraits of extra-solar systems using the current ground-based telescopes (5-10-meters). Exoplanets are roughly thousand to ten billion times fainter than their stars and finding such dim signals in the presence of overwhelmingly bright stars is technically challenging. Moreover, the light of a star-planet pair that traverses through the Earth is blurred by the atmospheric layers of different temperatures, humidity, and wind speeds. The structure of telescopes also vibrates due to the motion of motors and local wind, which collectively, makes it challenging to disentangle exoplanetary signals from the starlight. This makes direct imaging biased towards finding exoplanets that shine their own light and reside far away (farther than Sun-Saturn distance) from their parent stars. The first and foremost requirement for capturing signs of life is to find closer-in exoplanets by overcoming the technical challenges faced by state-of-the-art direct imaging instruments. In this talk, I will discuss how the current instruments overcome these challenges and acquire images of exoplanets.

Title: Detecting Wave Dark Matter with Pulsar Polarization and Timing Arrays
Speaker: Prof. Tao Liu from Hong Kong University of Science and Technology (HKUST)
Date: 27 January
Venue: UKZN Venue: Online SAAO Zoom
Time: 15h00

Abstract: Dark Matter (DM) is a long-standing puzzle on the Universe. Wave DM is one of the most representative theories to address this puzzle. In this talk, the speaker will introduce how pulsar arrays, which have been originally proposed to detect nanoHz gravitational waves as a galactic timing interferometer, stand at the frontier of detecting wave DM. The speaker will particularly address in this context: (1) the significance of developing "pulsar polarization arrays" (see https://arxiv.org/abs/2111.10615); and (2) the necessity of correlating pulsar polarization arrays (PPA) and pulsar timing arrays (PTA). The projected sensitivities form a great complementarity with the existing bounds on wave DM. The detection of wave DM thus defines one task of high scientific value for new-generation PTA/PPA programs

Title: What's in a shadow? Past, Present and Future of Black Hole Imaging
Speaker: Heino Falcke Radboud University Nijmegen
Date: 23 February
Venue: SAAO – Auditorium
Time: 11h00

Abstract: The inside of black holes is shielded from observations by an event horizon, a virtual one-way membrane through which matter, light and information can enter but never leave. This loss of information, however, contradicts some basic tenets of quantum physics. Does such an event horizon really exist? What are its effects on the ambient light and surrounding matter? How does a black hole really look? Can one see it? In 2019 we have made the first image of a black hole and detected its dark shadow in the radio galaxy M87 with the global Event Horizon Telescope (EHT). In 2022 the EHT, with crucial Dutch contributions, published the first image of the black hole in the centre of our Milky Way. Detailed supercomputer simulations faithfully reproduce these observations. Simulations and observations together provide strong support for the notion that we are literally looking into the abyss of the event horizon of a supermassive black hole. The talk will review the results of the Event Horizon Telescope, the nature and meaning of the black hole shadow, its scientific implications and future expansions of the array.

Title: A Laser Frequency Comb for SALT's High-Resolution Spectrograph
Speaker: Dr Lisa Crause, SAAO
Date: 22 February
Venue: SAAO Auditorium
Time: 19h30

Abstract: SALT is partnering with researchers in the UltraFast Optics group at Heriot-Watt University (HWU) in Edinburgh to build a laser frequency comb (LFC) for our high-resolution spectrograph (HRS). This state-of-the-art device will enable extremely precise wavelength calibration for the instrument's high-stability mode, a critical step towards equipping the HRS for exoplanet science. All of the many components required to build the comb have been procured and delivered to the SAAO over the past year. The project lead from HWU visited recently to test the equipment in Cape Town, then in April him and his team will travel to Sutherland to carry out the integration and testing at the telescope. This is an extremely exciting project for all of us, as this sort of interdisciplinary collaboration is a great opportunity for both camps to learn new things and potentially spark future innovations.

Title: A new constraint on modified gravity theories (plus more) from the anisotropic galaxy bispectrum"
Speaker: Ass. Prof Saito Shun, Missouri University of Science and Technology
Date: 24 February
Venue: UWC Room 1.35
Time: 11h00

Abstract: Everyone agrees that it is powerful to map out three-dimensional distribution of the large-scale structure through galaxy redshift surveys and intensity mapping surveys. Yet I argue that there could still remain interesting information in the 3D maps which everyone has not paid a close attention. In this talk, I will overview how useful the anisotropic component of the galaxy bispectrum is to constrain a class of modified gravity theories as well as the consistency relation of the cosmological density perturbation. Then I will show our recent results on our measurement from the galaxy catalogues in Baryon Oscillation Spectroscopic Survey.

Streicher Asterisms 101-106

Magda Streicher

STREICHER 101 – DSH J1856.2-3958

Corona Australis

What a beautiful group consisting of only five stars in a tight concentration. This one deserves to be named an asterism even has the looks of an open cluster and strongly outstanding against the visible starfield. The very faint galaxy PGC 625538 is situated a few arc minutes towards the west. It is situated in the middle area of the Coronae Australis constellation.

OBJECT	TYPE	RA	DEC	MAG	SIZE
STREICHER 101 DSH J1856.2-3958	Asterism	18h56m.15	-39°58'.17	8.5	2.8'

Picture Credit: Picture Credit: http://archive.stsci.edu/cgi-bin/dss

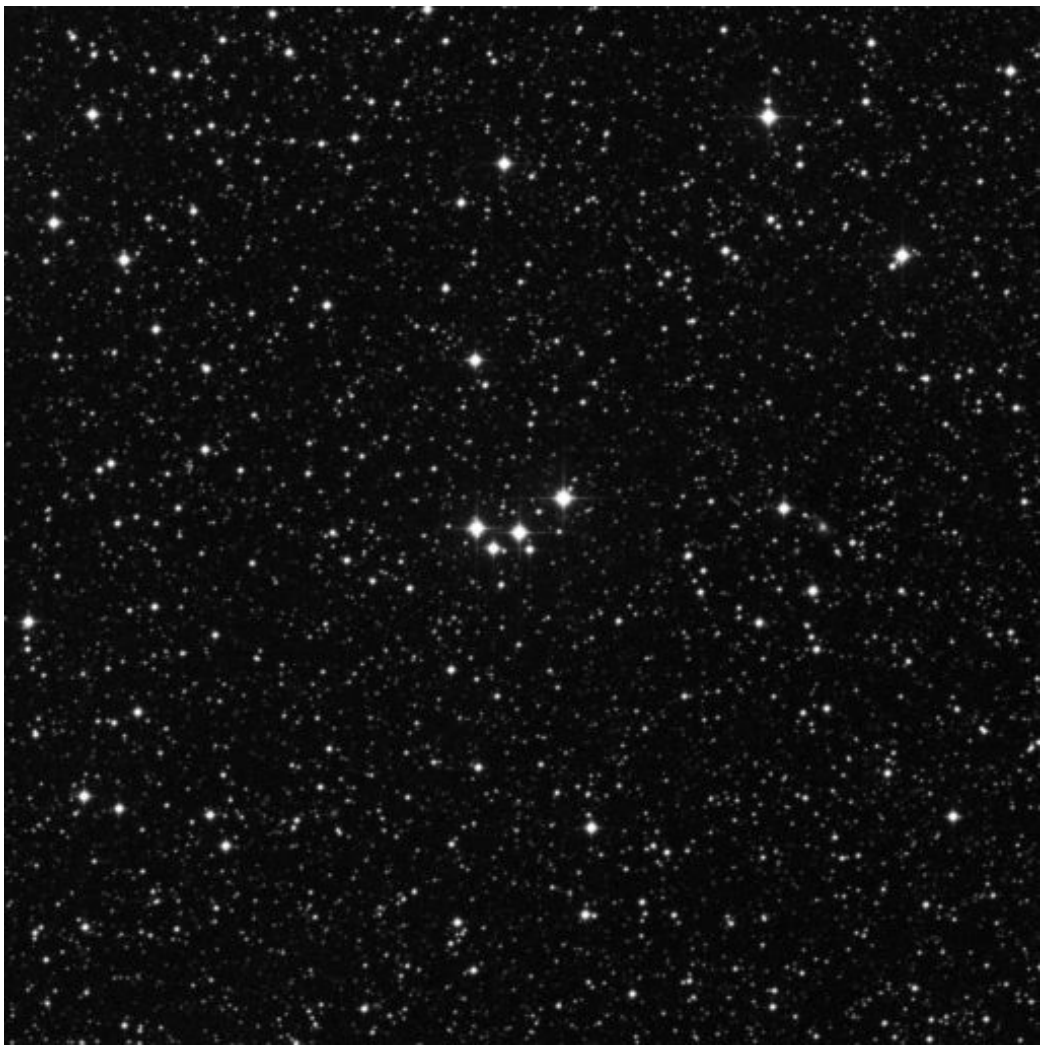

STREICHER 102 – J2102.5+0534

Equuleus

What a lovely grouping; quite outstanding with the brighter and striking magnitude 8.6 star the main focus covered in a colourful yellow jacket. Fainter stars of similar magnitude surrounds the northern and southern parts. Seen in another context the stars form a nice S-shape from north to south.

OBJECT	TYPE	RA	DEC	MAG	SIZE
STREICHER 102 DSH J2102.5+0534	Asterism	21h02m.27	+05°34'.12	11	6'

Picture Credit: http://archive.stsci.edu/cgi-bin/dss

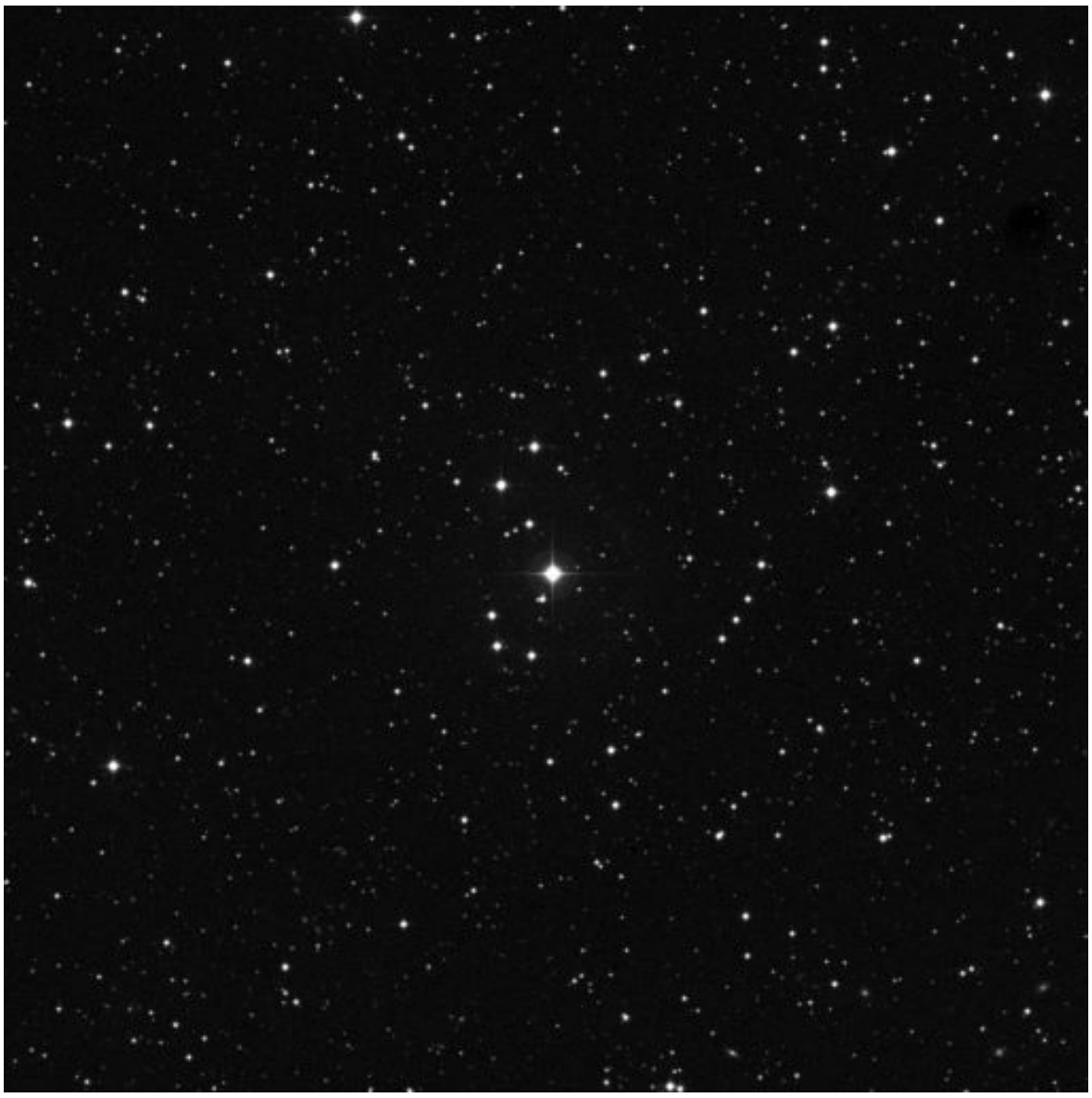

STREICHER 103 – DSH J0653.0+2216

Gemini

This special close grouping resembles a clear type of a dip V-shape. The star field around the asterism is gracious sprinkled with several faint stars. With a careful eye the faint galaxy PGC 19793 can be spotted just of the northern tip of the asterism as seen on the Deep Sky Survey picture. Asterisms are decidedly among the most exciting star groupings for launching a random search, look out for them with an open eye.

OBJECT	TYPE	RA	DEC	MAG	SIZE
STREICHER 103 DSH J0653.0+2216	Asterism	06h53m.02	+22°16'.06	10.3	11'

Picture Credit: http://archive.stsci.edu/cgi-bin/dss

STREICHER 104 – DSH J1557.5-3247

Lupus

Only four stars in this asterism but well lifted out against the star field, one to remember. Close investigation brings to light a very faint gathering of stars a few arc-minutes towards west as can be seen in the Deep Sky Survey picture below. The star Chi Lupi shines with a magnitude of 4 further south-west.

OBJECT	TYPE	RA	DEC	MAG	SIZE
STREICHER 104 DSH J1557.5-3247	Asterism	15h57m.27	-32°47'.09	9	3.2'

Picture Credit: http://archive.stsci.edu/cgi-bin/dss

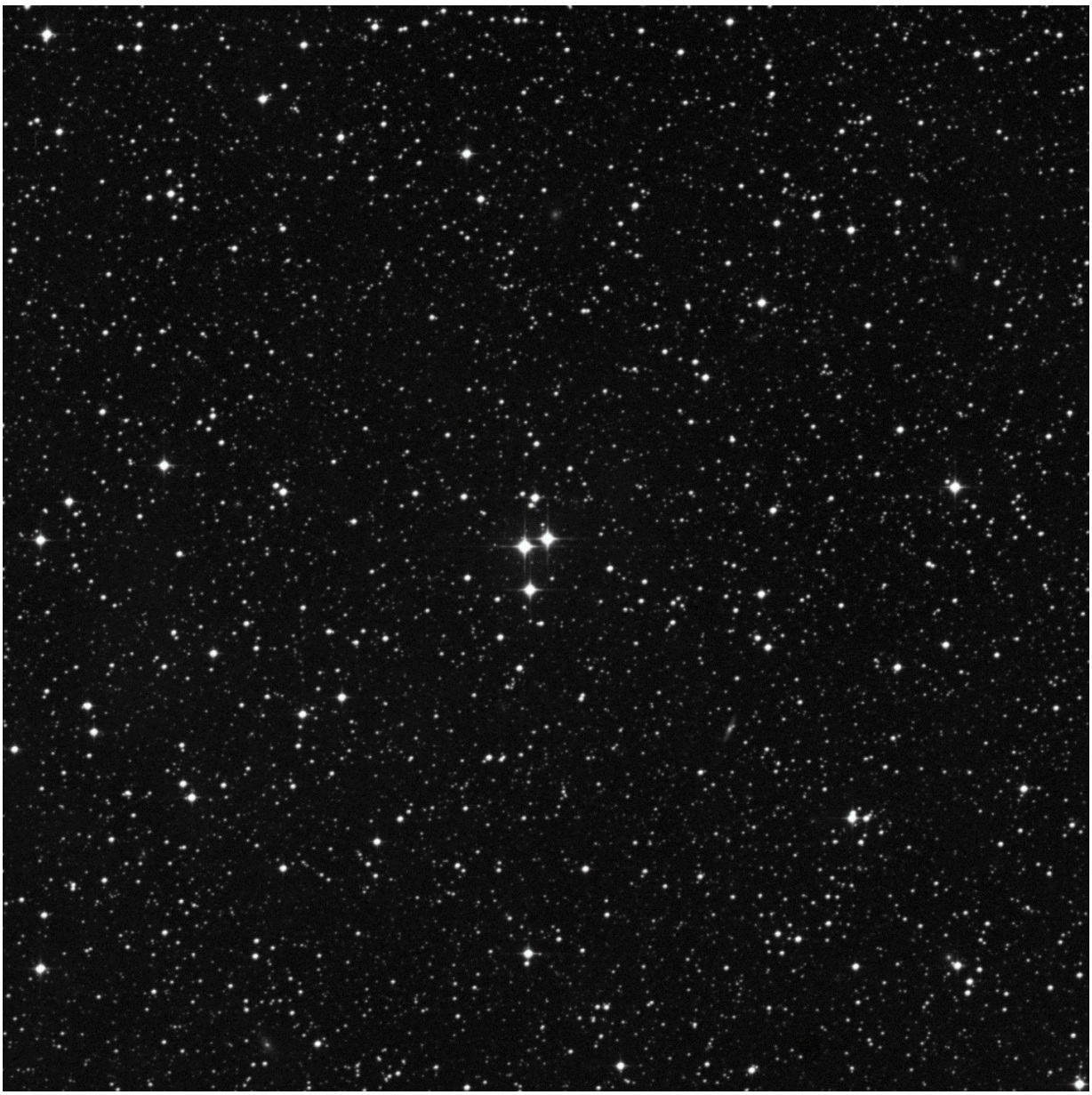

STREICHER – 105 DSH J1622.4-4446

Norma

What a wonderful find; a mist of very faint stars in a relatively tight group, with the looks of a real cluster seen against the background star field. The grouping is located in a triangle south-east from delta and lambda Norma. In an area dotted with faint stars it is difficult to spot groupings like this.

OBJECT	TYPE	RA	DEC	MAG	SIZE
STREICHER 105 DSH J1622.4-4446	Asterism	16h22m.24	-44°46'.06	12	1.8'

Picture Credit: http://archive.stsci.edu/cgi-bin/dss

STREICHER 106 – J1509.8-6925

Triangulum Australe

This tiny clump of stars hides itself in against a crowded star field. The group displays a roughly triangular shape somewhat difficult to lift out. Larger magnification brings to mind a type of V-shape. A few PGC galaxies are situated less than a degree north and north-west of the asterism.

OBJECT	TYPE	RA	DEC	MAG	SIZE
STREICHER 106 DSH J1509.8-6925	Asterism	15h09m.46	-69°25'.24	11.8	2'

Picture Credit: http://archive.stsci.edu/cgi-bin/dss

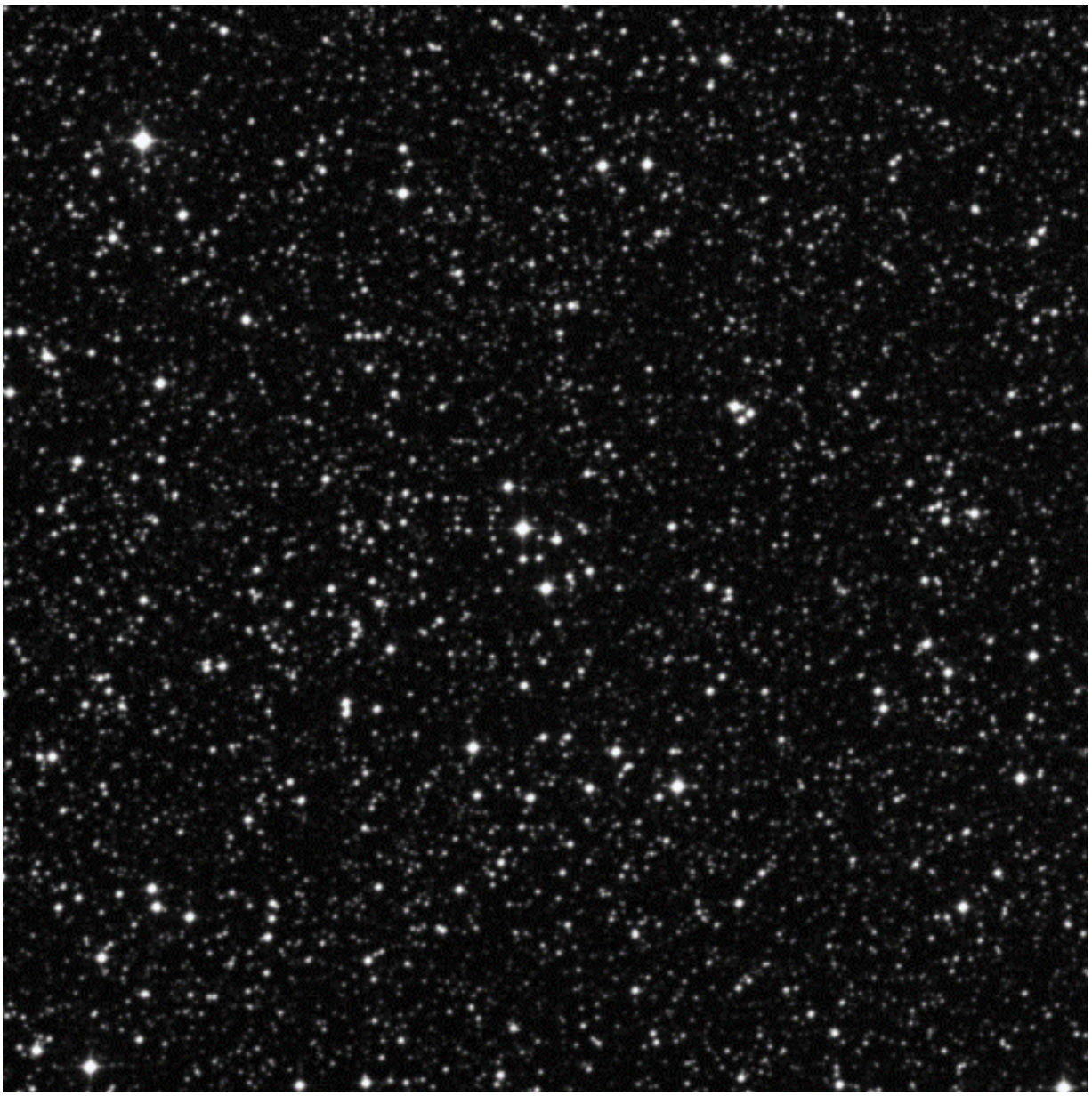

The **Astronomical Society of Southern Africa** (ASSA) was formed in 1922 by the amalgamation of the Cape Astronomical Association (founded 1912) and the Johannesburg Astronomical Association (founded 1918). It is a body consisting of both amateur and professional astronomers.
Publications: The Society publishes its electronic journal, the *Monthly Notes of the Astronomical Society of Southern Africa (MNASSA)* bi-monthly, the annual *Sky Guide Africa South* and *Nightfall*.
Membership: Membership of the Society is open to all. Potential members should consult the Society's web page : http://assa.saao.ac.za for details. Joining is possible via one of the local Centres or as a Country Member.
Local Centres: Local Centres of the Society exist at Bloemfontein, Cape Town, Durban, Hermanus, Johannesburg, Pretoria and the Garden Route Centre; membership of any of these Centres automatically confers membership of the Society.
Internet contact details: email: assa@saao.ac.za Home Page: http://assa.saao.ac.za

ASSA Council	
President	Dr Daniel Cunnama
Vice-President (outgoing)	Chris Stewart
Vice President (Incoming)	Dr Pierre de Villiers
Membership Secretary	Eddie Nijeboer
Treasurer	AJ Nel
Secretary	Lerika Cross
Council Member	Case Rijsdijk
Council Member	Dr Ian Glass
Bloemfontein Chair	Thinus van der Merwe
Cape Chair	Christian Hettlage
Durban Chair	Amith Rajpal
Garden Route Chair	Case Rijsdijk
Hermanus Chair	Derek Duckitt
Johannesburg Chair	Carmel Ives
Pretoria Chair	Johan Smit
Council Appointees	
Scholarships	Claire Flanagan
ASSA Communication Coordinator	Dr Sally MacFarlane
Webmaster	John Gill
Section Directors	
Dark Sky	Dr Daniel Cunnama
Observing section	Angus Burns
Photometry, Spectroscopy	David Blane (caretaker role)
Cosmology, Astrophysics	Bruce Dickson
History	Chris de Coning
Double and Variable Stars	Dave Blane
Imaging	Martin Heigan
Instrumentation and ATM	Chris Stewart
Comet, Asteroid and Meteor Section	Tim Cooper

ISSN 0024-8266

mnassa

monthly notes of the astronomical society of southern africa

Volume 82 Nos 1-2 **February 2023**

Table of Contents

News Note: Royal Astronomical Society announces all journals to publish as open access from 2024 1

News Note: International Team Announces Discovery of Super-Hot Stars Using Southern African Large Telescope 2

The 2022 campaign to observe potential meteors from asteroid Bennu 3

Some thoughts on Dobsonian telescope bearings 9

Darkness and colour of the Total Lunar Eclipses of 2022 18

Colloquia 32

Streicher Asterisms 101-106 36